CALIFORNIA ENERGY COMMISSION

Energy Research and Development Division

FINAL PROJECT REPORT

Self-Tracking Concentrator Photovoltaics

Gavin Newsom, Governor

March 2020 | CEC-500-2020-021

PREPARED BY:

Primary Authors:
Peter Kozodoy
John Lloyd

Glint Photonics, Inc.
1520 Gilbreth Rd., Burlingame CA 94010
650-646-4192
www.glintphotonics.com

Contract Number: EPC-14-040

PREPARED FOR:
California Energy Commission

Silvia Palma-Rojas, Ph.D.
Project Manager

Jonah Steinbuck, Ph.D.
Office Manager
ENERGY GENERATION RESEARCH OFFICE

Laurie ten Hope
Deputy Director
ENERGY RESEARCH AND DEVELOPMENT DIVISION

Drew Bohan
Executive Director

ACKNOWLEDGEMENTS

Glint Photonics, Inc. (Glint) is very grateful to the California Energy Commission (CEC) for their support of this work. As a small company, we could not have pursued this program without the funding provided by the CEC. In addition, CEC staff provided deep engagement in the project's technical and market aspects, providing valuable advice, encouragement, connections, and guidance throughout the program. Glint is especially grateful to the Commission Agreement Manager, Dr. Silvia Palma-Rojas, who provided detailed supervision and assistance throughout. In addition, the team is grateful to Rizaldo Aldas for his support of the program, and Janna Franks for assistance with legal and financial matters.

Glint also gratefully acknowledge support from the Advanced Research Projects Agency for Energy (ARPA-E) within the United States Department of Energy through awards DE-AR0000332, which laid the groundwork for the project described here, and DE-AR0000644, which helped support the research described here and provided cost-share. Glint's gratitude extends to the ARPA-E staff, including program directors Howard Branz and Michael Haney, tech-to-market advisers Kacey Gerst, James Zahler, and Graciela Blanchette, and technology staff Brian Borak, Zigurts Majumdar, and Marcus Bagnell. The team also gratefully acknowledge related SBIR funding that laid the groundwork for this project: NSF award IIP-1114079 and DOE award SC0009207.

Glint thanks the members of our Technical Advisory Committee, who provided valuable advice and insight: James Blatchford of California ISO, Howard Branz of Branz Technology Partners, Bob Hemphill of AES Solar Energy (retired), and Mark Henderson of Kinematics Manufacturing.

The team also wishes to thank numerous collaborators. These include Bill McMahon, Kelsey Horowitz, and Ryan France at the National Renewable Energy Laboratory (NREL), with whom we collaborated on PV cell optimization and module cost model development. They also include Matthew Meitl, who assisted in fabrication process development, and Adam Plesniak, who performed the third-party evaluation of our module performance and testing.

Finally, the authors thank the various other staff members at Glint who contributed to this research, including Kevin Bauer, Chad Casper, Victor Chub, Christopher Gladden, Andrew Kim, Barbara Kruse, Michael Pavilonis, Jeff Perkins, Christopher Rhodes, Kevin Schneider, Royal Wang, Toby Wheeler, and Emma Xu.

PREFACE

The California Energy Commission's (CEC) Energy Research and Development Division supports energy research and development programs to spur innovation in energy efficiency, renewable energy and advanced clean generation, energy-related environmental protection, energy transmission and distribution and transportation.

In 2012, the Electric Program Investment Charge (EPIC) was established by the California Public Utilities Commission to fund public investments in research to create and advance new energy solutions, foster regional innovation and bring ideas from the lab to the marketplace. The CEC and the state's three largest investor-owned utilities—Pacific Gas and Electric Company, San Diego Gas & Electric Company and Southern California Edison Company—were selected to administer the EPIC funds and advance novel technologies, tools, and strategies that provide benefits to their electric ratepayers.

The Energy Commission is committed to ensuring public participation in its research and development programs that promote greater reliability, lower costs, and increase safety for the California electric ratepayer and include:

- Providing societal benefits.
- Reducing greenhouse gas emission in the electricity sector at the lowest possible cost.
- Supporting California's loading order to meet energy needs first with energy efficiency and demand response, next with renewable energy (distributed generation and utility scale), and finally with clean, conventional electricity supply.
- Supporting low-emission vehicles and transportation.
- Providing economic development.
- Using ratepayer funds efficiently.

Self-Tracking Concentrator Photovoltaics is the final report for the Self-Tracking Concentrator Photovoltaics for Distributed Generation project (Contract Number EPC-14-040) conducted by Glint Photonics, Inc. The information from this project contributes to the Energy Research and Development Division's EPIC Program.

For more information about the Energy Research and Development Division, please visit the CEC's research website (www.energy.ca.gov/research/) or contact the CEC at 916-327-1551.

ABSTRACT

Concentrator photovoltaic systems provide more efficient solar energy generation than conventional solar panels by focusing sunlight onto small but highly efficient solar cells. However, these systems require special mounting on precision pivoting trackers to follow the sun. The resulting cost and complexity has precluded rooftop installation and prevented the technology from achieving significant market penetration. Glint's self-tracking concentrator photovoltaic system is a new design that eliminates the need for mounting on mechanical trackers. The system can provide the high-efficiency of concentrator photovoltaics in a flat, stationary, low-cost package that mimics a conventional silicon module, and can be mounted directly to commercial or residential rooftops or used with simple single-axis trackers.

Through this project, Glint Photonics developed this technology and evaluated its potential cost and performance. The team built three generations of prototypes, each of which achieved performance targets. Researchers operated a final prototype successfully for two months in a rooftop test. The prototype provided a module efficiency of 22.5 percent, similar to that of top-performing silicon panels. Optimized designs could can offer even higher efficiency. Cost and performance studies indicate that the technology could be especially valuable on area-constrained rooftops, where it could provide a higher capacity installation in the same physical footprint and share the balance-of-system costs, such as wiring, switches, battery bank, and solar inverters. However, further research and development would be required to enable higher technology and market readiness.

In addition to successfully demonstrating a new photovoltaic technology, the technical knowledge acquired in the project contributed to the development of two innovative energy-efficient lighting technologies that have strong commercialization opportunities and are the subject of ongoing research and product development efforts.

Keywords: concentrator photovoltaics, solar, PV, CPV, self-tracking, stationary

Please use the following citation for this report:

Kozodoy, Peter and John Lloyd. 2020. *Self-Tracking Concentrator Photovoltaics.* California Energy Commission. Publication Number: CEC-500-2020-021.

TABLE OF CONTENTS

LIST OF FIGURES

LIST OF TABLES

Page

EXECUTIVE SUMMARY

Introduction

Solar photovoltaic electricity generation provides clean renewable energy to meet California's energy needs. However, current silicon photovoltaic modules have low efficiency, converting only about 16 to 20 percent of the sun's power into electricity. Concentrator photovoltaics promise higher-efficiency solar energy generation at reduced cost. The basic principal is simple: use low-cost optical materials like lenses and mirrors to focus sunlight onto smaller solar cells. This reduces the amount of solar cell material required and allows for the use of higher cost multijunction cells with conversion efficiency above 40 percent. Conventional concentrator photovoltaic systems, however, require special mounting on precision pivoting trackers to follow the sun, and the resulting cost and complexity has prevented them from achieving significant market installations. It also makes them inappropriate for use in rooftop installations.

This project developed, improved, and tested early prototypes of the self-tracking concentrator photovoltaic system, an innovative concentrator photovoltaic design that eliminates the need for mounting on mechanical trackers by integrating an internal tracking solution. The system can provide the same high-efficiency benefits of large-scale concentrator photovoltaics in a flat, stationary, low-cost package that mimics a conventional silicon module, and can be mounted directly to commercial or residential rooftops or used with simple one-axis trackers. For the first time, such a system would allow the use of low cost concentrator photovoltaic in the distributed generation market, supporting California's goals of 60 percent of the state's electricity supplied by renewable energy by 2030. The systems would also support California's goals to make all new construction zero-net-energy by increasing the energy generation potential of constrained-area rooftops.

Project Purpose

This project provided a detailed evaluation of the potential cost and performance of the self-tracking concentrator photovoltaic system technology, and advanced its technology readiness level. The project results presented a clear view of how self-tracking concentrator photovoltaic system could offer a compelling commercial product, offering higher efficiency and lower costs than conventional photovoltaic technology. Further, the project aimed to reduce the technical risk through proof-of-concept prototype demonstrations. The ultimate goal was widespread commercial use of self-tracking concentrator photovoltaic system products to increase solar electricity production and lower energy costs for ratepayers.

This research addressed multiple audiences. One audience is technologists and investors within industry and the public sector, who would continue to invest in technology development. A second audience is the community of scientists, engineers, and researchers working on high-efficiency photovoltaic technologies, as sharing ideas and results can lead to new ideas, hybrid technologies, and more rapid progress as a community. A final audience is energy planners, policy makers, and analysts who keep abreast of early-stage technologies that could impact future energy systems.

This project:

- Developed optimized designs for self-tracking concentrator photovoltaic system systems.
- Developed fabrication procedures and a supply chain for self-tracking concentrator photovoltaic system prototypes meeting defined performance targets.
- Demonstrated the performance of self-tracking concentrator photovoltaic system prototypes through laboratory tests and installation at an operating test site.
- Analyzed the total energy savings and market potential of self-tracking concentrator photovoltaic system products.

Project Approach

The research in this project was carried out by the engineers and scientists at Glint Photonics, Inc. with input and support from numerous outside experts. The project team worked with scientists at the National Renewable Energy Laboratory on photovoltaic cell design and cost modeling, and with several vendors on developing custom components and fabrication processes. The project leveraged separate funding and technical support from the United States Department of Energy Advanced Research Projects Agency-Energy. Experts on the technical advisory committee provided market insight and helped in selecting from design options.

Technical research included design work, process development, prototype fabrication, and prototype testing. The design effort was carried out using computational modeling of optical, thermal, and electrical properties to evaluate candidate designs toward optimized designs. Process development involved experimental work on the fabrication process for the self-tracking concentrator photovoltaic system modules, including evaluation of materials, development of assembly protocols, and testing of different mechanical and electrical schemes. The team fabricated three generations of prototypes, as the designs and fabrication processes matured. Each generation of prototypes targeted more aggressive performance specifications. The team used a solar simulator to perform indoor testing of the prototypes in Glint's laboratories and carried out outdoor testing in the solar testbed installed on Glint's rooftop. Testing of the final prototype module on the roof lasted for several months and included an electrical load to simulate real-world operation.

Glint carried out cost and performance analysis, developing a computer program to project the annual electrical energy output from self-tracking concentrator photovoltaic system modules in different geographical locations. The team compared these values to similar simulations for conventional silicon modules. The analysis used preliminary cost models for eventual self-tracking concentrator photovoltaic system products to estimate the technology's levelized cost of electricity in comparison to silicon modules, for a range of installation types and locations.

Several challenges emerged during the project. The first was to narrow the technical approach, as the team considered several potential optical architectures and designs for stationary mounting and mechanical tracking. Glint's team undertook early optical modeling and system performance analysis to explore this large design space and met with the technical advisory committee to discuss the results. This process helped identify the most promising technical approach and narrowed the focus to the design best suited for stationary mounting. In the ensuing experimental work to realize the design, the researchers faced many fabrication challenges, as is typical in prototyping work. These were due to factors such as custom mechanical parts that were out of specification, adhesives that failed, materials that warped or cracked, or electrical connections that failed. These challenges were overcome with a mix of creative engineering, close work with suppliers, and late nights in the laboratory.

Project Results

The project successfully achieved its objectives. The project team built and tested the three generations of prototypes, and all met or exceeded their target performance. In extended outdoor testing, the final prototype provided consistent performance and demonstrated a peak electrical conversion efficiency of 22.5 percent, similar to the top performing silicon modules.

The performance analysis suggested that optimized modules might achieve a total real-world energy conversion of 26 percent for the year, exceeding the performance of silicon modules. The self-tracking concentrator photovoltaic system technology remains at an early stage of development, despite the significant progress made in this program. Additional research might be focused on improving mechanical aspects of the system, exploring scaling to larger module sizes, developing a deeper understanding of the impact of soiling and other forms of environmental degradation, developing a design for mass manufacturing, and undertaking larger pilot installations.

Further research should also focus on the cost of eventual self-tracking concentrator photovoltaic system products, especially because the modules are more complex than silicon modules. With current cost estimates, the self-tracking concentrator photovoltaic system do not provide a cost benefit over silicon in dollars per watt. This questions the viability for utility-scale installations, where module cost is a dominant concern, and will even make adoption on area-constrained rooftops difficult. Further research might focus on quantifying the commercial opportunity with a more detailed cost modeling approach.

The team recommends future research on the self-tracking concentrator photovoltaic system project focus primarily on addressing cost and scalability. The team also recommends that product development be centered on rooftop and other area-constrained applications, where the high efficiency of the self-tracking concentrator photovoltaic system is particularly valuable.

A number of research challenges stand out for continued technology development of the self-tracking concentrator photovoltaic system module design including:

- Module designs to mitigate bowing and ensure accurate vertical positioning of optical elements.
- Exploration of manufacturing challenges relating to module scale-up. Larger modules will reduce overall system costs by leveraging motors and mechanics across a larger area.
- Cost reduction and simplification of actuators and mechanical design for micro-tracking.
- Development of module-scale micro-tracking control circuitry.
- More extensive pilot testing and environmental exposure testing.
- Critical evaluation of soiling impact.
- Detailed cost and performance model development.

Technology/Knowledge Transfer/Market Adoption (Advancing the Research to Market)

During this project, Glint shared technical progress with the research community through presentations at a number of scientific conferences and publication of journal articles. The researchers intend to continue sharing the final results through new publications and presentations. Glint also presented the results multiple times at the Advanced Research Projects Agency-Energy forum, a venue that draws a mix of scientists, policy makers, investors, and industry players. Further, the team has engaged privately with investors and companies interested in the technology.

The likely first market for self-tracking concentrator photovoltaic system products is in rooftop solar installations, or perhaps other niche area-constrained applications such as forward military bases. Regardless, the technology requires more research and development to develop cost-attractive high-efficiency products that can compete with conventional silicon modules. Glint will continue to explore opportunities to secure further funding or to adapt the technology to specific photovoltaic opportunities.

The novel optical and mechanical architecture developed in this project also has useful application in the lighting field. The work performed and technical knowledge obtained have led to the development of innovative lighting technologies and contributed to two new research projects at Glint: solar concentrator optics to provide daylighting in building interiors, and a similar optics paired with light emitting diodes (LED) to provide novel adjustable high-efficiency lighting fixtures. Both offer substantial energy savings impact and have strong commercial opportunities due to the design and functionality benefits they offer. Glint has secured research funding for both and is pursuing research and development opportunities. The steerable lighting technology was publicly revealed in 2018, and a first LED lighting product, the Hero adjustable tracklight/downlight, was announced in 2019 and will be commercially available in 2020.

Benefits to California

Successful development of self-tracking concentrator photovoltaic system modules would bring a number of benefits to California ratepayers. The team estimates a potential of 66 gigawatts (GW) from California rooftop installations, producing 92 terawatt hours (TWh) of electricity annually. This is approximately 40 percent of California's total annual electricity consumption, worth more than $11 billion.

Peak solar energy production by self-tracking concentrator photovoltaic system systems would coincide with times of peak demand, and the team estimates that full adoption of self-tracking concentrator photovoltaic system on California rooftops would offset 84 percent of peak demand. It would also reduce greenhouse gas generation by 30 million metric tons (carbon dioxide equivalent [CO_2e]), using the emissions factor of 0.331 kilograms CO_2e per kilowatt-hour provided by the Energy Commission's Energy Research and Development Division staff.

Significant benefits will also accrue from the related technologies in daylighting and LED lighting. Solar daylighting products bring natural sunlight into building interiors, offsetting electricity use for electric lighting and reducing the heating, ventilation, and air conditioning load. Complete adoption of daylighting products within California could save 1,523 gigawatt hours (GWh) annually and reduce greenhouse gas generation by 403,000 metric tons (CO_2e).

Glint's configurable LED lighting products save energy by providing more precise and adaptable illumination in occupied spaces and increasing the adoption of efficient, long-lasting LED-based luminaires. When paired with smart controls and sensors, Glint's dynamically-adjustable lighting technology will target illumination where it is needed as room use changes, with a resulting increase in end-use energy efficiency that could save up to 16.3 TWh annually in California. This amount of energy savings corresponds to 5.4 million metric tons of CO_2 emissions avoided.

Both lighting technologies also provide intangible benefits, by bringing high-quality lighting to interiors and providing better lighting distribution. This provides direct benefits to California residents in well-being, productivity, and safety.

In addition to these benefits, the successful development of this technology could bring significant manufacturing employment opportunities to California. Unlike conventional photovoltaic modules that are primarily built overseas, self-tracking concentrator photovoltaic system modules are well-suited to local manufacturing because they do not benefit significantly from co-location with the semiconductor foundry. Concentrator photovoltaic cell technology is an area where United States manufacturers have a substantial technical advantage over foreign competitors, including California companies such as Spectrolab and Solar Junction.

CHAPTER 1: Introduction

Motivation

The adoption of distributed photovoltaic (PV) generation has been limited by high soft costs (such as installation), which make up over half the installed system cost. Increasing the efficiency of distributed PV generation technology is an attractive way to leverage these soft costs and bring down the total system expense on a per-Watt basis. The highest efficiency PV cells are multijunction PV cells used in concentrator photovoltaic (CPV) systems, which offer >40 percent conversion efficiency (compared to ~ 16 percent for polycrystalline silicon (Si). Conventional CPV systems, however, require special mounting and precision tracking, and the resulting cost and complexity has so-far prevented them from achieving significant market penetration. An ideal solution for distributed generation would be one that provides the high conversion efficiency of CPV but without significant added balance-of-systems costs.

Concentrator photovoltaics have long promised higher efficiency solar energy generation at reduced cost. The basic principal is very simple: use inexpensive optical materials like lenses and mirrors to focus sunlight onto smaller solar cells. This reduces the amount of solar cell material required and allows for higher efficiency solar cells to be used. These systems have suffered historically however because of the precise tracking requirements. At typical high concentrations (>100x), the system must track the sun within a fraction of a degree. The cost and complexity of maintaining tight alignment tolerances and using precision tracking machinery can easily outweigh the benefits resulting from reduced solar cell usage and increased efficiency. Furthermore, precision trackers are generally bulky heavy devices requiring special foundations and are therefore poorly suited to most distributed-generation sites.

The aim of this program was to develop, test, and demonstrate Self-Tracking Concentrator Photovoltaic (ST-CPV) systems, a new solar energy concentrator that allows concentrator photovoltaic (CPV) system with high concentration and little or no mechanical movement of the module. The system can provide the same high-efficiency benefits of large-scale concentrator photovoltaics in a small, stationary, low-cost package that can be mounted directly to commercial or residential rooftops or used with simple 1-axis trackers in distributed generation.

Such systems would enable for the first time the deployment of low cost CPV in the distributed generation market. It would support California’s goals for renewable distributed generation as well as the Renewables Portfolio Standard, which sets continuously escalating renewable energy procurement requirements for the state’s load-serving entities. The systems would also support California’s goals to make all new construction zero-net-energy by increasing the energy generation potential of constrained area rooftops.

Background

The limitations of conventional CPV have spurred interest in novel stationary high-concentration CPV architectures. In such designs, the focusing optics remain stationary and small-scale internal adjustments in the optical system provide the required sun-tracking ("micro-tracking"). Stationary CPV panels are designed using close-packed arrays of small-scale focusing optics. This configuration can provide thin flat panels that mimic the form factor of conventional flat-plate photovoltaic (PV) modules, and that can be mounted similarly using standard racking. If sufficiently low-cost in their construction, stationary CPV panels can provide a new type of high-efficiency alternative to conventional PV modules in locations with high direct normal incidence (DNI).

The optical design approach was initially developed by Professor Joseph Ford at the University of California San Diego (Karp, J.H., 2010). This early work inspired a variety of approaches using a focusing lens arrays with different architectures and different mechanisms for achieving micro-tracking (Baker, K., 2012; Schmaelzle, P.H., 2010; Zagolla, V., 2012; Zagolla, V., 2014). A variant using combined lens and mirror arrays was investigated also by the Ford group (Ford, J.E., 2011) and more recently by the Giebink group at Penn State (Price, J.S., 2015). These two design approaches form the foundation of the design and prototype work undertaken in this project.

Glint Photonics, Inc (Glint) began development of stationary concentrator designs in 2012, with a system that used thermally-driven fluid motion to achieve micro-tracking. This work, initially funded by the Department of Energy's Advanced Research Projects Agency—Energy (ARPA-E), led to initial designs and proof-of-concept prototypes that served as the foundation for this project. Follow-on funding through the ARPA-E Micro-scale Optimized Solar-cell Arrays with Integrated Concentration (MOSAIC) program ran concurrently with this Energy Commission project, providing cost share and accelerating the technical progress.

Project Objectives

- Develop optimized designs for ST-CPV systems.
- Develop fabrication procedures and a supply chain for ST-CPV prototypes meeting defined performance targets.
- Demonstrate the performance of ST-CPV prototypes through both laboratory tests and installation at an operating test site.
- Analyze the total energy savings and market potential of ST-CPV products.

Project Approach

The project was organized around six technical task areas.

1. Optimization of ST-CPV designs. Design studies were performed using computer simulations of the optical, thermal, and electrical performance. The team considered a number of design approaches, as the early proof-of-concept designs provided only a narrow range of incident light angles for high-efficiency operation. For the same reason, the team considered three potential mounting configurations. In the first configuration, panels are mounted without any tracker (Figure 1). In the second configuration, panels are mounted on simple single axis trackers either on the roof or on the ground (Fig. 1b), which allows for higher energy capture and a reduced range of incident light angles that the panel must capture, but comes at the cost of some additional complexity. In the third configuration, the panels are mounted on simple, low accuracy two-axis tracking systems. This design can capture the most energy and places the least optical challenge on the concentrator design, but brings additional complexity and cost. The project team concluded that only the stationary configuration is truly suited for rooftop implementation, so the aim was to develop design approaches that would permit high efficiency operation in this configuration. The team achieved this aim and developed the selected design for stationary mounting through the remainder of the program.

Figure 1: Mounting Options for Self-Tracking Concentrator Solar Photovoltaic Modules

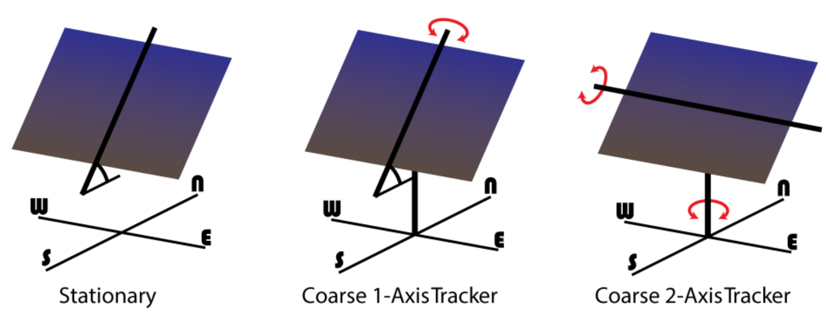

Source: Glint Photonics Inc., 2019.

2. Develop detailed cost/performance models for ST-CPV systems. These models combine detailed cost models with technical analysis to predict annual energy generation of the systems. The team analyzed the predicted cost/performance of the systems across different locations in California (and the rest of the United States) and compared to state-of-the-art silicon modules. The results helped drive design decisions and approach.
3. Process development. A large portion of the project was devoted to experimental work in developing fabrication procedures for the ST-CPV systems. The team performed this work in laboratory facilities at Glint and involved a wide range of

process steps and close collaboration with outside vendors providing custom parts or services. In this task, the team evaluated fabrication processes both for near-term prototype builds and long-term manufacturing.

4. Prototype fabrication. The prototyping effort encompassed three generations of prototypes, each built to achieve predetermined targets for size, optical efficiency, and feature set. Prototype fabrication took place in the Glint laboratories, with parts fabricated both in-house and through outside vendors.
5. Prototype module testing. The team tested the prototypes in-house at Glint using a highly collimated Class AAA solar simulator[1] and used the results to analyze performance of the prototypes, identifying issues and feeding information back into the design and fabrication cycles. The researchers developed testing protocols to evaluate angular acceptance, internal heating, environmental stability, and more.
6. Prototype system testing. In the final task, the team installed an optimized prototype module on the roof at Glint's facility for extended outdoor testing and attached the module to a load to mimic real-world conditions. This outdoor testing allowed extensive data collection on system performance, allowing analysis of power conversion efficiency under a wide variety of illumination conditions, as well as optical efficiency, internal heating, and the effect of soiling and other environmental exposure. In addition, a third-party expert inspects the test and measurement setup to validate the approach.

Performance Targets

The statement of work lays out specific performance targets for the three generations of prototype modules. The definition of the key metrics and terms used within this report are below:

- Annual Capture Fraction (ACF) (percent) measures the optical efficiency of the concentrator system. It is defined as the total annual light captured by the concentrator system and delivered to the solar cells divided by the total direct solar resource available for the year for a given location and mounting/tracking configuration.
- Standard Annual Capture Fraction (S-ACF) (percent): Annual Capture Fraction for a specific location and mounting configuration used as a standard for comparing performance. The standard used here is a module mounted stationary in Bishop CA, facing due South and tilted at latitude, with a clear hemispherical view of the sky.

[1] A class AAA solar simulator meets the highest specifications for spectral content, spatial uniformity, and temporal stability according to International Electrotechnical Commission (IEC) 60904-9 Edition 2 and ASTM E927-10 standards.

- Standard Test Condition (STC): Test condition for evaluating module performance. STC is defined as direct sunlight incident at an intensity of 1000 watt per square meter (W/m^2) normal to the beam, Air Mass 1.5 Direct (AM1.5D) spectrum.
- Optical efficiency (percent): Fraction of the direct sunlight incident on the module that reaches the PV cell.
- Direct-Current (DC) module efficiency at STC (percent): DC electrical power produced by the module divided by input optical power, when operated at Standard Test Condition
- Annual Energy Production (AEP) (kWh/m^2): Total direct-current (DC) energy generation over the course of the year for a given location and installation type. This is a particularly useful metric for comparison to conventional technologies in constrained area applications.
- Energy Harvest Efficiency (EHE) (percent): Total DC energy generation over the course of the year divided by total solar energy incident on the panel over the course of the year. The denominator includes both direct sunlight (accessible by the system) and indirect (not accessible). This metric provides a useful comparison to conventional flat-plate PV in the same configuration, as conventional PV can access both direct and indirect sunlight. It is the true in-use average module DC efficiency.
- Capacity Factor (percent): Actual energy output of a module as a fraction of nameplate capacity. This is calculated as AEP for a given location and mounting configuration, divided by the (DC module efficiency at STC * 1000 W/m^2 * 24 hours * 365 days)
- Levelized cost of electricity (LCOE) (¢/kWh): This is a system level metric that represents the total cost of a system divided by total kWh produced over its planned lifetime. The team calculated LCOE using a tool developed by the National Renewable Energy Laboratory (NREL), which is described in detail in Chapter 5.

For the stationary mounting case pursued in this work, the optical performance targets for the prototypes are listed in Table 1.

Table 1: Optical Performance Targets for Prototype Modules

Prototype Generation	Minimum Size (inches)	Minimum STC Optical Efficiency	Minimum S-ACF
Gen 1	4” x 4”	30%	15%
Gen 2	12” x 12”	40%	25%
Gen 3	12” x 12”	55%	45%

Source: Glint Photonics Inc., 2019.

In addition to these optical targets, the statement of work specifies the system-level performance targets listed in Table 2.

Table 2: System Performance Targets

Parameter	Minimum Value
DC Module Efficiency at STC	22%
Projected capacity factor (Bishop, CA)	14%

Source: Glint Photonics Inc., 2019.

CHAPTER 2:
Evaluation of Technological Approaches

Two CPV module designs were under consideration in the early part of the project. Both designs use small-scale arrayed optics in a flat module configuration, and both aim to reduce the need for external tracking of the module by implementing internal micro-tracking mechanisms. However, the two designs differ in optical characteristics and micro-tracking approach. This chapter describes the two approaches, with evaluation of the achievable performance for each design and the associated fabrication challenges. The evaluation ultimately led to a decision to abandon the first design (the "singlet design") developed in the prior research work described in Chapter 1, and pivot instead to the second design (the "catadioptric design"), which offered a more compelling opportunity for high-performance modules.

Singlet Optical Design With Fluidic Self-Tracking

As shown in Figure 2 on the far left, a slab light-guide is covered by an array of *mm*-scale lenses that concentrate incoming sunlight to form an array of focal spots near the bottom face of a slab light-guide. The slab is clad on the top by a passive low-refractive-index material (e.g. a fluoropolymer), and on the bottom by a thin (5 to 30 micron) layer of light-reactive optical cladding. The entire structure is approximately 2 to 10 millimeter (mm) thick. To form a self-tracking concentrator, coupling of the focused light into the guide must be made to occur automatically at the focal spots, in a way that follows movements of the focal spots with the changing angle of solar incidence. The design for self-tracking uses thermocapillary forcing in a microfluidic configuration. Compared to prior efforts, it has the advantages of actuating at low incident power and being largely insensitive to environmental temperature.

Figure 2: Rendering of Singlet ST-CPV Device Geometry (left) and Operation (right) with the Fluidic Coupling Region of the Device

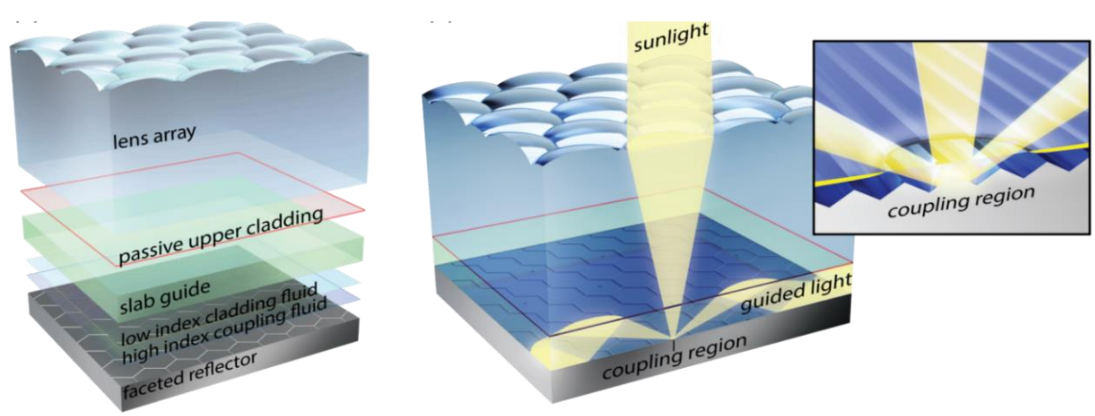

Source: Glint Photonics Inc., 2019.

As shown in Figure 2, a fluid bilayer forms the “smart” or “light-reactive” lower cladding material. This is constructed of a low refractive index cladding fluid that preferentially wets the slab surface, layered above an immiscible liquid of high refractive index, referred to as the coupling fluid. The fluids are held in place by a network of thin grid walls which separate the coupling fluid into individual droplet volumes so that capillary forces dominate over gravitational forces. Heating generated by the focused light produces a local reduction in interface tension between the two liquids, and the resulting thermocapillary forces deform the fluid interface, locally rupturing the low-index fluid layer and allowing the high-index fluid to provide a continuous high-index optical path between the guide and the underlying faceted reflecting surface. These “coupling regions” are dynamically generated at the focal point and will follow movement of the focal point as the solar position changes over time, thus providing automated tracking.

Focused light striking the facets at these coupling regions is deflected into angles that are trapped by the slab guide, and then travels through the guide by total internal reflection. Light from all the lenses is coupled into a common light-guide, and propagation loss is low because the thermally-generated coupling regions occur over only a very small fraction of the slab surface (typically less than 0.1 percent), with the remaining area clad by the low-index fluid. Concentrated light is extracted onto PV cells attached to the edge of the slab.

Experimental concentrator devices of this design were fabricated at a size of 1″ x 1″. Analysis of fluid response dynamics tested with focused laser illumination match predictions of the multi-physics simulation with high accuracy. The devices achieved optical efficiencies as high as 72 percent, and self-tracking at angles up to ± 25° in the axis parallel to the coupling facets. Angular response of one prototype concentrator device is shown in Figure 3. This wide self-tracking range greatly exceeds the narrow acceptance angle of conventional concentrating optics, and is sufficient to track the seasonal elevation change of the sun.

Figure 3: Optical Efficiency of Singlet Concentrator Prototype

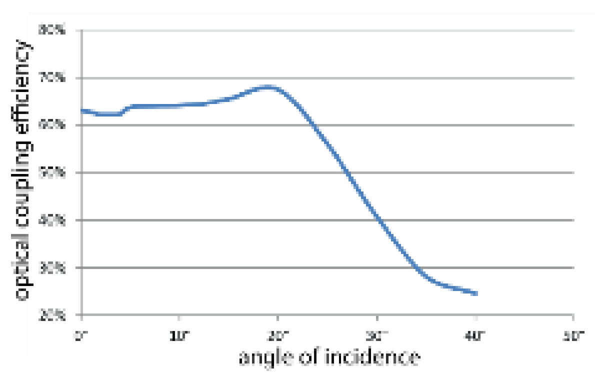

Source: Glint Photonics Inc., 2019.

Angular acceptance in the other axis is lower, due to focal plane curvature of the focusing optics (as shown in Figure 4) and reduced coupling efficiency into the guide for off-axis reflections from the facets. Thus, the singlet optical design is only practical for implementation on a platform with at least some coarse mechanical tracking in one axis.

Figure 4: Off-Axis Focusing Characteristics of an Optimized Singlet Lens

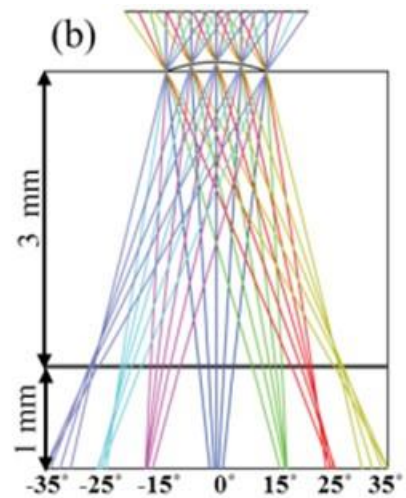

Source: Glint Photonics Inc., 2019.

Because the optical properties of the concentrator vary depending upon the incident light characteristics, system design optimization is a complex problem requiring coupled analysis of optical, fluidic, and thermal properties over the anticipated range of illumination conditions. Simulations to determine optimal designs have been undertaken, combining multiphysics finite-element analysis and non-sequential raytrace modeling within a computational framework that iterates the performance analysis over the range of light incidence angles and intensities expected in a given location and mounting configuration over the course of the year. Table 3 shows the analysis for a system located in Tucson, Arizona (AZ), but similar results would be expected for systems in high DNI locations within California. Performance will be worse in low-DNI locations.

Table 3: Calculated Performance of Optimized Singlet Concentrator Systems

Mounting	Geometric Concentration	ACF in Tucson, AZ
Coarse 2-Axis Tracker (10° accuracy)	750x	68.2%
Tilted 1-Axis Tracker	400x	58.5%
Horizontal 1-Axis Tracker	150x	46.1%
Stationary	100x	35.5%

Source: Glint Photonics Inc., 2019.

Two trends in this data are interesting to note. Both reflect the limitations of the singlet design in effectively capturing wide-angle light and show its poor performance as the degree of mechanical tracking is reduced.

The first trend is that optimal system designs provide lower concentration levels as the degree of mechanical tracking is reduced. Singlet systems optimized for mounting on a coarse two-axis tracker have the highest performance and most design flexibility, since they are able to maintain tightly defined focal spots all the time. These systems can achieve high concentration levels, with an optimum system analyzed at 750x geometric concentration. Singlet systems on single-axis trackers do not maintain such tight focal spots, and therefore must sacrifice some concentration to maintain reasonable optical efficiency. This tradeoff is even more severe for stationary systems.

The second trend is decreasing ACF as the degree of mechanical tracking is reduced. This stems primarily from the curved focal plane of the single lens element and the inability to effectively focus light on a planar surface over a wide range of angles.

The conclusion drawn from this evaluation was that, despite its potential to be manufactured at very low cost performance, this design is ultimately a non-starter for stationary mounting due to the low ACF. Acceptable ACF was only achieved when paired with a two-axis tracker, which was expected to significantly limit market acceptance.

Catadioptric Optical Design

The catadioptric design, as shown in **Error! Reference source not found.**, uses a front refractive lens and a back reflective lens to form a focus between the two optics. The use of the combined optics allows for the focal plane to be flattened and eliminates the majority of chromatic aberrations. Focused light may be aggregated in a central lightguide, but improved efficiency is achieved by placing arrayed solar cells on a transparent substrate suspended at the focal plane, and mechanically translating the sheet inside the cavity. This optical structure enables high efficiency light gathering out to incident angles of ~ 70º in both axes, with only small translational "micro-tracking" movements of the transparent sheet. This design is therefore fundamentally well- suited to realization of stationary CPV modules. However, the optical design introduces various practical challenges.

The first of these was to achieve the required micro-tracking of the central sheet. Unlike the singlet system, in which movement of fluids alone can provide the required optical changes for tracking, tracking in the catadioptric design requires physical movement of a solid object. This entails larger forces, although still orders of magnitude lower than in conventional two-axis mechanical trackers. It is possible to provide self-tracking orientation of solid objects via thermofluidic effects driven by focused sunlight, however initial research was unable to produce sufficient force to effectively reposition the sheet within the module. Many other actuation schemes are also possible using embedded low-cost actuators; the slow short-throw low-force requirements of the system are compatible with a variety of electromagnetic, thermoelectric, and piezoelectric actuator types.

Figure 5: Design and Operation of the Catadioptric Concentrator System

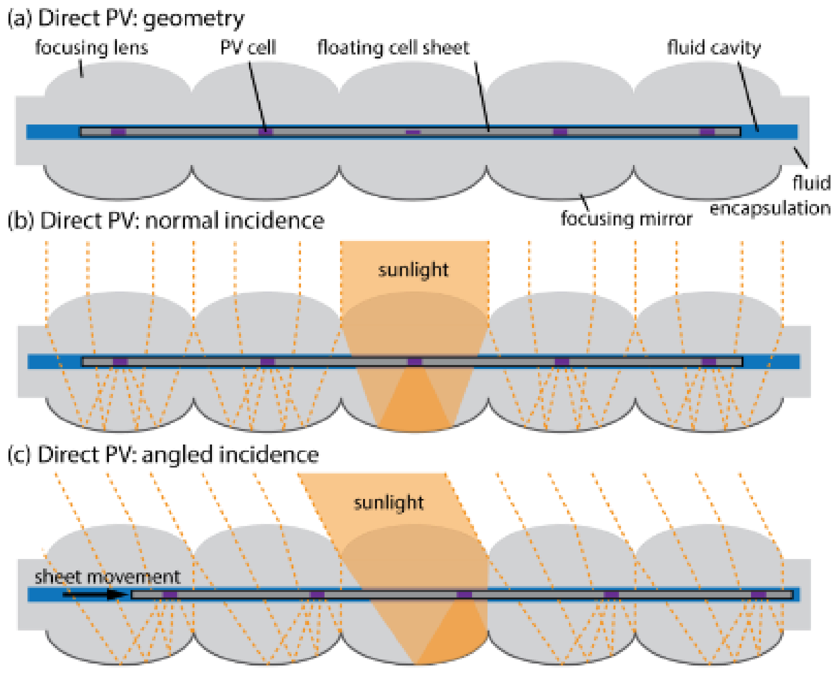

Source: Glint Photonics Inc., 2019.

A second complication was the requirement to mount the cells on a transparent sheet. This precludes the use of conventional backplane materials. The researchers developed designs to prevent registration errors resulting from thermal expansion differences between the glass or polymer sheet and the molded polymer optics. Such errors can result from environmental temperature variation as well as self-heating effects during operation.

A third complication was in PV cell heat mitigation. Conventional heat-sinking approaches cannot be used for the cells due to the requirement for optical transparency. The transparent polymer sheet and fluid ambient have low thermal conductivity, so heat removal is primarily via the metal traces connecting the cells, with a tradeoff between heat removal and shadowing impact. Narrow but vertically thick metal traces are optimal. The design provided further improvements by using a network of traces that provide effective heat spreading in the area between PV cells.

The optical performance of an initial candidate catadioptric system design was evaluated using non-sequential raytrace analysis software. Figure 6 shows a sample design and raytrace analysis. This initial design provides 260x concentration at the focal spot, with optical efficiency as a function of incident angle as shown in Figure 7. The design maintains high optical efficiency to incidence angles of 50°. The performance of this design was analyzed for each of the four mounting configurations, and in each of the six locations within California. The analysis used typical meteorological year (TMY) data from the NREL TMY3 dataset in 1-hour increments. The ACF data is presented in Figure 7.

Figure 6: Raytrace Analysis of Example Catadioptric System.

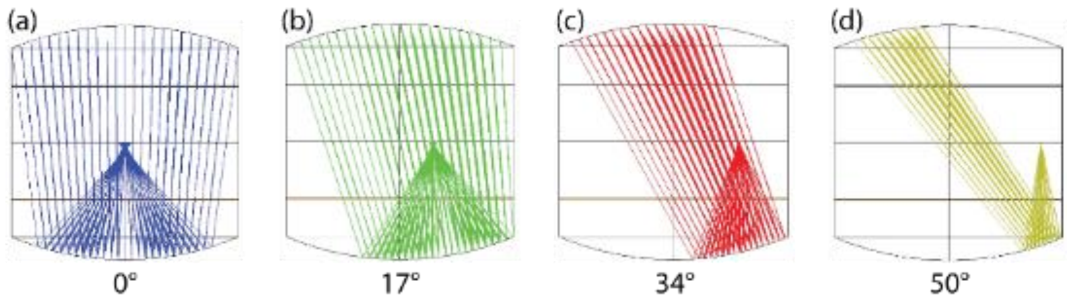

Source: Glint Photonics Inc., 2019.

Figure 7: Optical Efficiency of G1 Design as a Function of Light Incidence Angle

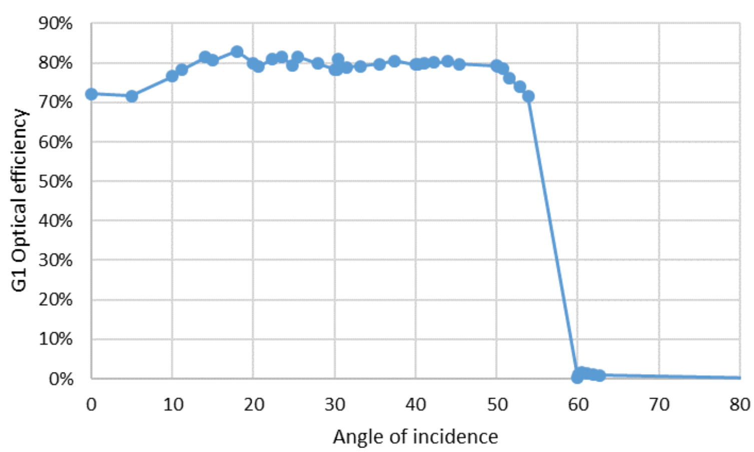

Source: Glint Photonics Inc., 2019.

Table 4: Calculated ACF Values for Initial Catadioptric Design in Various Mounting Configurations and Locations

Location	Stationary	Horizontal 1-axis	Tilted 1-axis	Coarse 2-axis
Oakland	70.0%	76.5%	78.4%	71.6%
Burbank	69.4%	77.1%	78.5%	71.6%
Long Beach	70.6%	77.2%	78.5%	71.6%
San Diego	70.8%	77.5%	78.4%	71.6%
Bakersfield	69.0%	77.2%	78.5%	71.6%
Bishop	68.5%	76.4%	78.4%	71.6%

Source: Glint Photonics Inc., 2019.

The ACF values vary very little between location, as ACF is a relative measure (how much of the locally-available DNI is captured). Because the performance of the catadioptric design is largely insensitive to incident power levels, the ACF is not strongly affected. Of course, actual energy production for CPV panels will vary significantly with location due to the variation of direct solar resource.

Mounting on a single-axis tracker provides higher ACF than stationary mounting, because the mechanical tracker improves the system’s ability to capture light shining at high angles at the beginning and end of the day. A tilted one-axis tracker provides only modest improvements over a horizontal tracker. Use of a dual-axis tracker actually reduces ACF performance because the design has lower efficiency near 0° incidence.

It is clear from this analysis that the catadioptric design shows very significant performance advantages over the singlet design, with high optical efficiency over a very wide range of incident light conditions that enables use in stationary mounting. The team decided to pivot experimental work to the catadioptric design only, and to focus on stationary mounting configurations.

CHAPTER 3: Prototype Design and Fabrication

Process Development

The project team developed three generations of prototypes, with increasing complexity. The Gen 1 prototype intended to validate the optical design approach with the simplest possible construction. It is smaller in size, containing only a single glass tile, and without a sophisticated mechanical drive system for micro-tracking. The Gen 2 prototype utilized large scale molded optics and served as the platform for developing the mechanization and electrical interconnect design, as well as developing key processes for assembling, sealing, and dosing the module. The Gen 3 module was the final product of this work, combining optimized design and processing in a fully-functional module for extensive on-sun testing.

Motorization

Module designs incorporated off-the-shelf commodity motors to drive internal micro-tracking via a mechanical drivetrain. This approach minimizes the execution risk in demonstrating the core optical architecture of the module within this program. Ultimate optimization of the actuator approach falls outside this program, but would involve considerations of precision, compactness, longevity, and cost, and should consider piezoelectric materials, shape memory alloys, and electromagnetic systems.

Tile Fabrication

The design strategy was to mount the PV cells on sheets made of glass, rather than a transparent polymer. This decision minimized execution risk, as considerable process development was needed to realize printed circuits and PV cell die attach on a polymer substrate. To mitigate thermal expansion differences with the polymer optics array, the design uses glass tiles of limited size, placed within an acrylic carrier tray.

Copper electrical traces were electroplated onto the glass tile and capped with Ni/Au to facilitate wire bonding between the cell top contacts and the electrical traces. In addition to two electrode arms per cell to extract photocurrent, heat spreading arms were incorporated to laterally spread waste heat generated at the cell to maintain lower device operating temperatures. Conservative fabrication constraints limited the aspect ratio of these features to 0.5:1 (thickness: width) but increasing this ratio would improve the heat spreading without significant optical penalties.

Triple-junction photovoltaic cells measuring 1.2 mm square were attached to the sheet using reflow soldering of the bottom contact. A wire-bonding process provided connection to the cell top contact. These cells provide a nominal conversion efficiency of 37.5 percent under AM1.5D illumination. All cells were electrically connected in parallel on the sheet, a circuit topology that protects mismatched photocurrents from cells from damaging reverse bias conditions.

Optics

The team sourced the lens arrays out of acrylic via compression molding (Gen 1) or injection molding (Gen 2). The rear optic was coated with a silver reflector layer in a vacuum coating process. The fabrication of these parts must consider precise tolerances to ensure proper registry of the top and bottom arrays, and correct total thickness to avoid future degradation of the optical performance. This proved to be a challenge, especially for the larger parts which exhibited some warpage and thickness error only partially mitigated through process improvements developed in conjunction with the molding vendor.

Prototype Fabrication

Gen 1 Prototype Construction

The Gen 1 prototype module had an optical aperture of 109 square centimeters (cm^2) containing 42 hexagonally packed unit cells. The lens diameter was 20mm and the geometric concentration ratio was 180x. The prototype assembly consisted of three-dimensional (3D) printed framing, a refractive front optic array, a reflective back optic array, an acrylic carrier with photoactive tile, and a sealing gasket as shown in Figure 8.

Figure 8: Gen 1 Prototype Exploded Assembly (top left), View of the Photoactive Tile Mounted in Acrylic Carrier With Embedded Magnets in Blue (right), and Prototype Under Test (bottom)

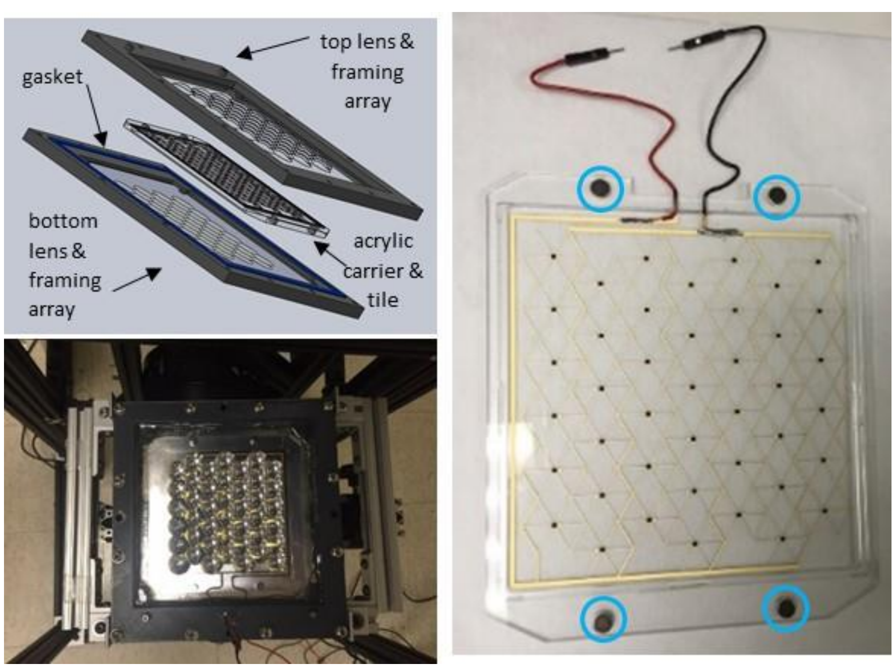

Source: Glint Photonics Inc., 2019.

The framing, when bonded to the lens arrays, served to align the lens arrays as well as provide a sealable fluid cavity for the photoactive tile. The acrylic carrier featured embedded magnets, to provide a mechanism for micro-tracking actuation. The tile could be positioned using a matching set of magnets on the exterior of the sealed module, which would pull the tile into alignment, allowing fine control over positioning.

The photoactive tile consisted of a glass tile with metalized copper traces, to serve as an electrical network for the photovoltaic cells. The trace layout was designed with electrical, optical, and thermal considerations in mind.

Electrical traces with successively larger widths were chosen to handle larger cumulative photocurrent while maintaining minimal resistive losses. To maximize optical performance, traces followed the contours of lens edges to minimize shadowing losses. Although only two metal traces are needed to provide electrical connection to each cell, additional traces were incorporated as heat spreaders to facilitate the movement of heat from the solar cell into the surrounding fluid. High efficiency triple junction cells are then soldered to the network of connections to convert the focused light into photocurrent. Wires soldered to the tile transited the gasket, providing connection to external measurement equipment.

Figure 9: Image of the Trace Layout Including Heat Spreaders and Electrically Active Traces (left) and Close Up of Attached High Efficiency Solar Cell (right)

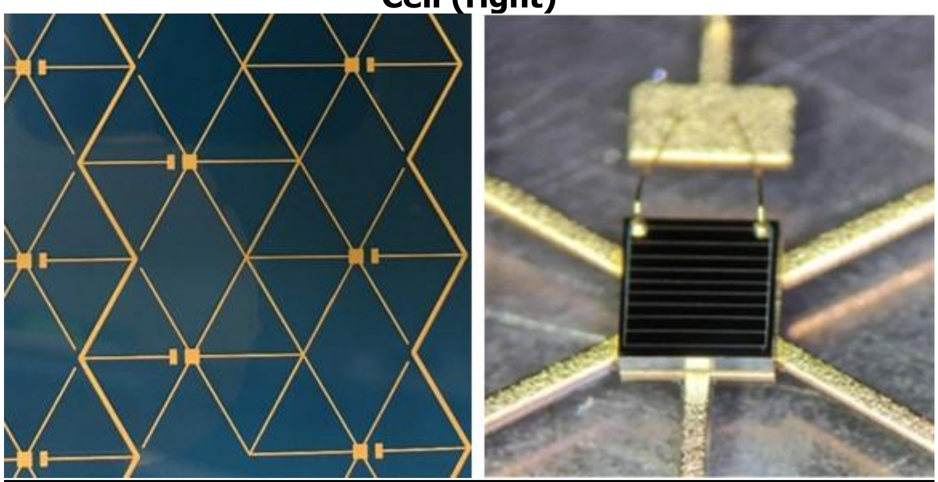

Source: Glint Photonics Inc., 2019.

Gen 2 Prototype Construction

The Gen 2 prototypes shared a common optical architecture with the Gen 1 prototypes. That architecture involved two molded lens arrays that form a catadioptric system: a front array that is refractive and a rear array that is reflective. The two lens arrays were positioned in registry with a thin gap between them in which photovoltaic cells are arrayed on receiver tiles, facing downward to accept the focused light emanating from the rear reflective lens array. The receiver tiles were immersed in a transparent fluid that is index matched to the lens arrays to prevent Fresnel reflections at interfaces. The tiles are placed in an acrylic carrier that can hold up to four tiles and ensures that all tiles are held in registry. The Gen 2 platform is approximately five times the aperture area of the Gen 1 platform. The lens arrays contain 363 lens units, each measuring 15mm x 20mm. The rectangular aperture of the lenses was chosen to correlate with the asymmetric angular range of incidence for stationary mounting: a wide range of incidence angles in one axis (East-West), and narrower in the second axis (North-South). The full module aperture dimensions are 280 mm x 390 mm. The geometric concentration ratio is 208x.

Figure 10: Schematic of Gen 2 Module Design

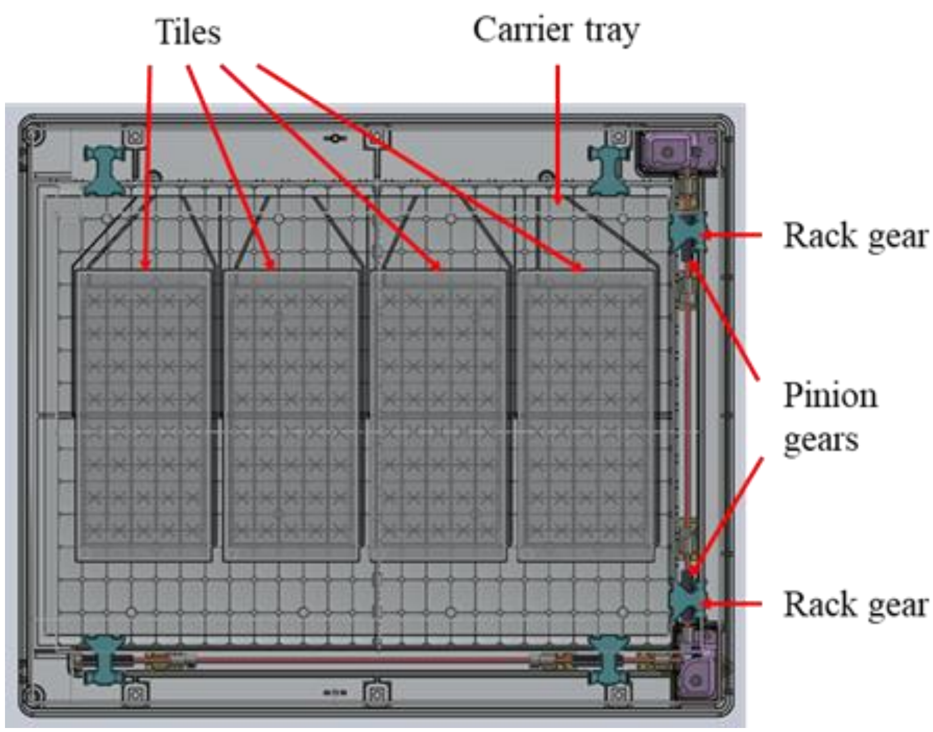

Source: Glint Photonics Inc., 2019.

The Gen 2 module also implements a full mechanical system for tile positioning. Two independent rack and pinion gearings drive the orthogonal translation axes of the receiver tiles, as shown in Figure 11. The gears are driven via stepper motors mounted outside of the module seal, with torque transmitted into the module via two magnetic clutches. This system allows for precise positioning in two independent axes with very low wear of the mechanical system. The rack and pinion system was constructed using off-the-shelf gearing combined with custom-manufactured shaft and collar, and a number of in-house 3D-printed parts to assemble all components and maintain alignment. Optimization of the mechanical drivetrain and motor mounting was a significant project requiring multiple prototype iterations.

Figure 11: Photo of Rack and Pinion Mechanics in Gen 2 Module

Source: Glint Photonics Inc., 2019.

The approach to seal Gen 2 prototypes was to attach the front and back lens arrays with a sealant designed for adhesion to acrylic and for outdoor applications. A tongue and grove seal is potted with sealant and provides a very thin but robust seal. Fluid is then dosed through small dosing ports, which are themselves then potted and sealed. Testing of evaluation modules confirmed the long-term durability of this critical seal. A sealed lens unit exposed on the rooftop for one year showed no change, and thermal cycling testing on sealed modules in the laboratory likewise showed robust performance.

Figure 12: Photo of Completed Gen 2 Prototype

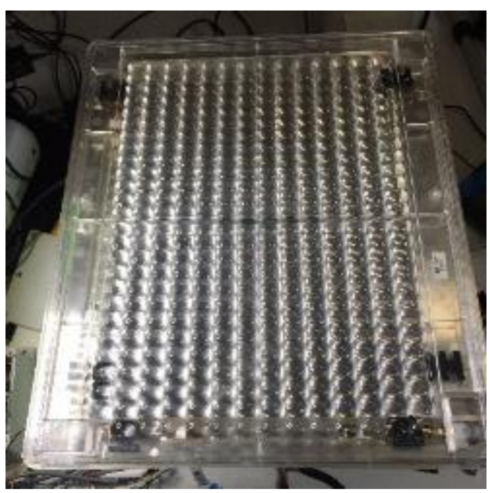

Source: Glint Photonics Inc., 2019

Gen 3 Prototype Construction

The Gen 3 prototype design is very similar to the Gen 2 design but involved a redesign of the acrylic tile carrier tray to allow for more efficient routing of bussing wire, as well as a sliding electrical contact design. These two improvements allowed for easier fabrication and ensured low resistance and robust electrical connection to the translating PV cells.

Figure 13 shows the revised carrier tray design. The design of the Gen 2 carrier included four tiles within the module, each tile having stranded wire soldered to it and routed through channels in the carrier tray. Unfortunately, the tiles were very fragile and soldering stranded wire to the tiles and routing it through small channels in the carrier tray was a challenging fabrication step. The revised carrier tray accommodates three tiles, and included wider channels designed for solar bussing wire rather than stranded wire. The solar bussing wire, which is pre-tinned with solder, is much easier to solder in place within the carrier, making fabrication and assembly simpler and easier.

Figure 13: Carrier Tray Design for Gen 2 (left) and Gen 3 (right)

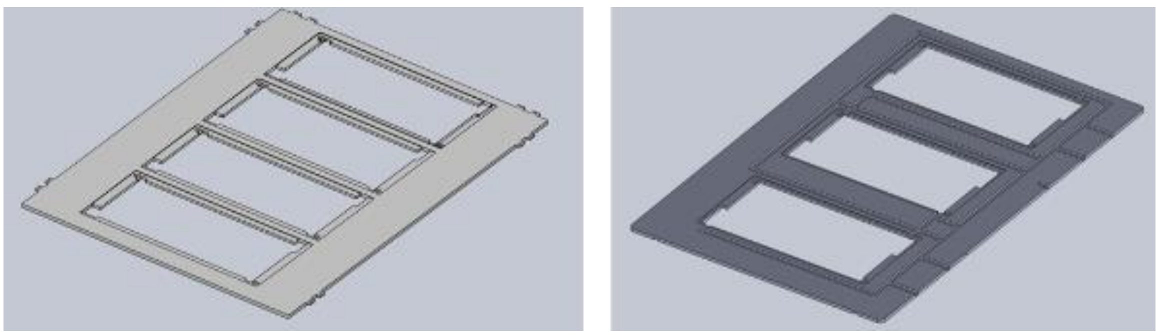

Source: Glint Photonics Inc., 2019.

The sliding contact scheme replaced the moving wires used in the Gen 1 prototype and some Gen 2 prototypes. These had to be routed with enough slack to accommodate movement with minimal strain and created a tradeoff between the wire resistance and mechanical compliance. Further, the moving wires required significant space within the module, and are subject to eventual fatigue failure.

The sliding contact scheme shown in Figure 14 provided reliable electrical connection at low resistance. It consists of multiple interleaved strips of solar bussing wire, specifically four strips soldered together and embedded within the carrier tray that slide between five other strips soldered at their ends and affixed to the module shell. This created eight interfaces that were constrained in both vertical directions while retaining mechanical compliance. Measurement of the electrical resistance indicated <10 milli-ohm (mΩ) even in the presence of the index matching oil ambient within the module, an acceptably low contact resistance that would not contribute significantly to the total module series resistance.

Figure 14: Close-Up of the Interleaved Bussing Wire Sliding Contact

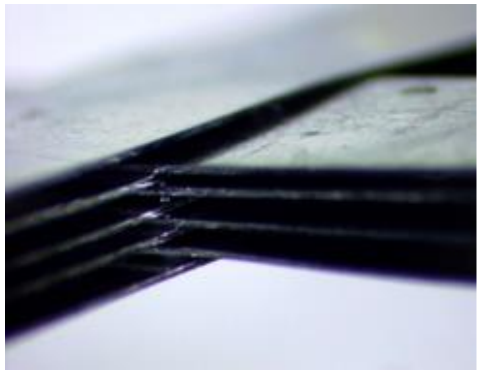

Source: Glint Photonics Inc., 2019.

The Gen 3 module suffered from a slow leak of fluid at the dosing port and was cleaned and refilled at one point during outdoor testing. This leak was very likely the result of reusing optical components from previous modules to work around vendor delays. The lens arrays used in this module were taken from an earlier gen 3 module and the mechanics were upgraded internally. The project team noted in previous experiments that the sealant does not work as well when parts are reused, likely because residual fluid impairs sealant adhesion. This is not inherent to the design, and other modules that were not resealed have been installed outdoors for months without sign of leakage.

Manufacturability and Supply Chain

In assessing technology viability it is important not only to demonstrate technical capability but also to identify any components or process steps that represent major challenges to manufacturability or supply chain. The team investigated realistic volume manufacturing processes and suppliers for a hypothetical module design based on this technology but built for mass-manufacturing. Key steps in the fabrication and associated supply chain are listed below. While some supply elements are not yet in place, no elements appear to be fundamental roadblocks to eventual commercialization.

High-Efficiency Multijunction PV Cells

High-efficiency multijunction PV cells are currently manufactured by a small number of suppliers, primarily for use on satellites. Terrestrial CPV can be supplied by this existing industry, and there is considerable capability to ramp production if needed. Cell costs are high currently, but technical pathways to significantly reduced cell cost have been studied and appear feasible, if driven by a substantial market for low-cost terrestrial CPV systems.

Fabrication of Tile Circuit Board

Processes used for conventional printed-circuit-board fabrication are applicable to building the tiles in volume. These include lamination, photo-definition, and etching/plating. Some retooling would be necessary for a conventional printed circuit board line to operate on a glass substrate, but circuit boards on glass have been built before for other products and this is a scalable process.

Attachment and Connection of Multi-Junction Photovoltaic Cells

Reflow soldering is the preferred mechanism for volume manufacturing, as it attaches all cells in a parallel process and provides optimal thermal and mechanical properties. In volume manufacturing, PV cell placement would likely be via pick-and-place tool. This approach provides sufficient placement accuracy, but is still a serial process and a non-trivial component of the total estimated module cost. Potential mechanisms for parallel placement of cells are worth evaluating in the long-term. These include multi-head "chip-shooter" versions of pick-and-place machines, as well as more exotic approaches such as transfer printing.

Wire bonding can be provided via automated machinery for low-cost high-volume production. Alternatively, it may be possible to design the PV cells with same-side contacts so that they can be attached in a single surface-mount step without requiring wire bonding.

Fabrication of Molded Optics Arrays

Injection molding remains the preferred manufacturing path at high volume. Indeed, it becomes much more economical with volume, as the high cost of the tool is amortized over the many parts it can produce at low per-part cost (the stainless steel tools typically last > 1 million copies). A critical issue will be maintenance of optical tolerances in the molded parts at large part dimensions, a challenge that will require careful process control in the injection molding operation.

Coating of Back Optic Array

Vacuum deposition will likely remain the preferred method of coating the back optic, even at high volume. At volume, investment in dedicated tooling and fixturing will help keep the cost of this step reasonable. An alternative approach is solution-deposition of coatings, which could provide significant cost savings if sufficient optical quality can be achieved.

Assembly and Seal

Assembly and seal processes will need to be automated for high-volume manufacturing. This will be achieved using custom-configured industrial machinery and fixturing, such as is typically used in automating assembly tasks.

CHAPTER 4: Prototype Testing and Evaluation

Prototype Testing

Laboratory Testing Setup

The project team performed the indoor tests of optical efficiency med at Glint using an Oriel 94123A-CPV Sol3A collimated solar simulator with an AM1.5D spectral filter. The module was mounted on a plate attached to a two-axis telescope tracker head which was driven to an incident test angle. The module was maintained at zero bias and the generated photocurrent was monitored in real-time on a Keithley 2420 source-measurement unit while the carrier position was manually optimized. At the position of peak photocurrent, a current-voltage trace was taken. Lamp output was normalized by measurements of the receiver tile removed from the module.

Optical efficiency is the fraction of photocurrent produced by the module at short circuit to the total potential photocurrent available in the incident light from the solar simulator. This metric ignores any efficiency penalty due to the photovoltaic conversion in the solar cells and provides a simple way to compare optical performance in each prototype build.

Power efficiency is a relative metric comparing the power produced by the panel operating at its max power point to the total power available in the incident light from the solar simulator. This encompasses all losses of the module and is the most important metric when comparing to existing technologies.

Figure 15: Glint Solar Simulator with Tip/Tilt Stage Below Optical Output

Source: Glint Photonics Inc., 2019.

The team used the measured values of optical and power efficiency as a function of incident light angle to extrapolate the estimated module performance for a given location based on the time-dependent DNI resource for that location, using NREL's TMY database. Per the scope of

work, performance is analyzed using this model and assuming a module mounted in Bishop CA, facing south at latitude tilt, for comparison to target values.

Gen 1 Prototype

Gen 1 Prototype Optical Performance

Table 5 shows the measured optical and power efficiency for the Gen 1 prototype as a function of incident light angle. Both efficiencies are reported as fractions of the DNI light, to readily compare with other existing CPV technologies. The optical efficiency values are in excellent agreement with the optical models for this system design and show effective capture of light from a wide range of incidence angles. The optical efficiency remains above 50 percent above the design target of 50º from normal. The module power efficiency is consistent with the expected performance of the 3-junction PV cell utilized considering the elevated operating temperature resulting from the indoor test conditions.

Table 5: Gen 1 Prototype Angularly Resolved Optical and Power Efficiency Efficiencies

Angle	Optical Eff	Power Eff
0°	76.3%	24.7%
10°	79.0%	26.3%
20°	74.4%	24.8%
30°	70.1%	23.1%
40°	62.3%	20.4%
50°	56.7%	18.5%
60°	42.8%	13.6%

Source: Glint Photonics Inc., 2019

Table 6 identifies the target performance metrics for the Gen 1 prototype vs achieved values.

Table 6: Target and Achieved Performance Metrics for Gen 1 Module

Metric	Target	Achieved
Aperture Area (sq inches)	16	16.9
STC Optical Efficiency	30%	76.3%
S-ACF (Stationary, Bishop)	15%	60.3%

Source: Glint Photonics Inc., 2019.

Gen 1 Prototype Tracking Performance

While laboratory testing of the prototype demonstrated excellent performance of the optical design, as documented above, the Gen 1 prototype design experienced a significant challenge. The translational magnetic coupling used to actuate the photoactive tile, while functional, is handicapped by stiction and hysteresis. As a result, the tile movement was jumpy and unpredictable. In laboratory testing, this was compensated for by manual adjustments to optimize the tile placement, bringing the photovoltaic cells into alignment with the focal spots and permitting measurements of module performance capability. But when tested outdoors with automatic tracking enabled, tile placement could not be well controlled and module output was typically only a fraction of what was expected based on the laboratory measurements of performance capability.

Gen 2 Prototype

Gen 2 Prototype Optical Performance

The Gen 2 prototype was tested at incident angles up to 70° under collimated irradiance from a solar simulator. This prototype module included two receiver tiles each with independent electrical connection so that they could be measured independently. Figure 16 depicts the optical efficiency of the centermost tile, which shows an unexpected functional form. The optical efficiency rose from approximately 40 percent at normal incidence to a peak of over 60 percent at 50° incidence in the long optical axis. The optical system as designed exhibits peak optical efficiency at normal incidence, with slowly decaying optical efficiency out to about 50°.

Figure 16: Optical Efficiency of Gen 2 Prototype Module with Incident Angle in the Long Axis

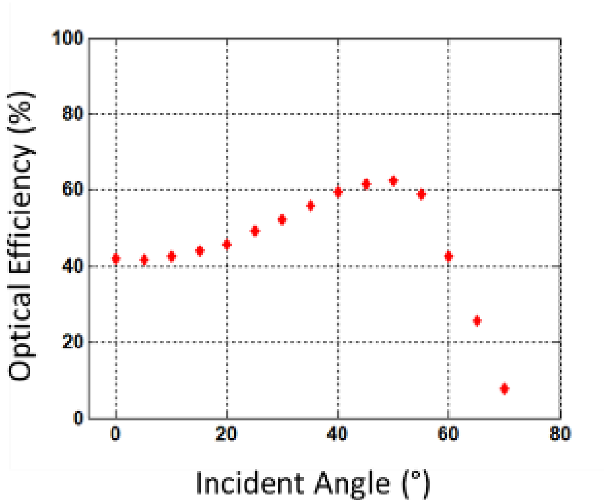

Source: Glint Photonics Inc., 2019.

The large Gen 2 lens arrays exhibited some bowing in the center of the module, and the distance between the front and back lens arrays was possibly not tightly matched to the optical design. The team performed ray-tracing simulations to verify the performance impact of increasing distance between the front and back lens arrays, and these simulations provided an excellent match to the functional form of the measured performance data. Figure 19 reports this data. Additionally, the molded back lens arrays are observed to contain approximately 0.5 mm of additional flange thickness that effectively increases the optical path length and defocuses the photovoltaic cells.

The team conducted repeated measurements with a crossbar clamped across the rear of the module to reduce any bowing of the back-lens array, resulting in significant improvement to the measured optical efficiency. Notably, the measured optical efficiency transformed from matching simulations consistent with a 5 mm cavity to matching simulations consistent with a 4.5 mm cavity. This is consistent with 0.5 mm of bowing and 0.5 mm of additional molded part thickness. Figure 18 depicts a repeated measurement of a Gen 2 module tile without and then with external clamping, showing a marked improvement with clamping.

Figure 17: Simulated Gen 2 Optical Efficiency With Increasing Separation Between the Front and Back Lens Arrays

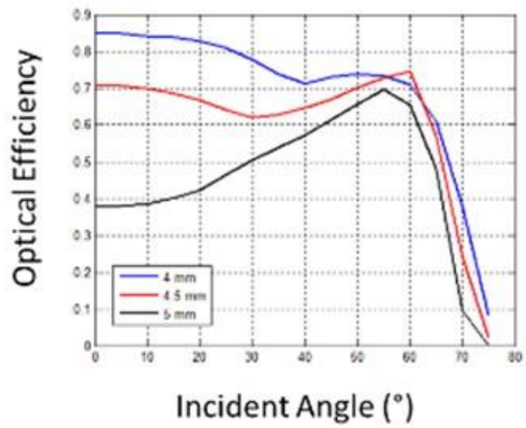

Source: Glint Photonics Inc., 2019.

Figure 18: Measured Optical Efficiency of a Tile in a Gen 2 Module With No External Clamping (left) and External Clamping (right)

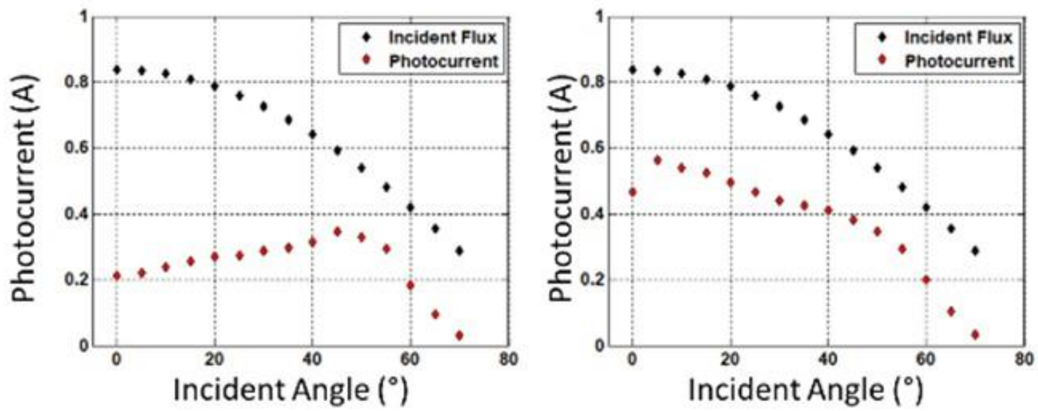

Source: Glint Photonics Inc., 2019.

A second Gen 2 module built with the thinnest of the available molded optics parts and clamped during optical testing yielded the improved optical efficiency data plotted in Figure 19. Table 7 shows the target performance metrics for the Gen 2 prototype vs achieved values. The performance of the Gen 2 module exceeds both the STC and S-ACF targets, showing the excellent optical properties of even these initial prototypes, despite the known problem of optical system bowing. The S-ACF value of 63.2 percent exceeds the value of 60.3 percent achieved on the Gen 1 prototype, despite the much larger size of the Gen 2 module.

Figure 19: Optical Efficiency of Improved Gen 2 Module

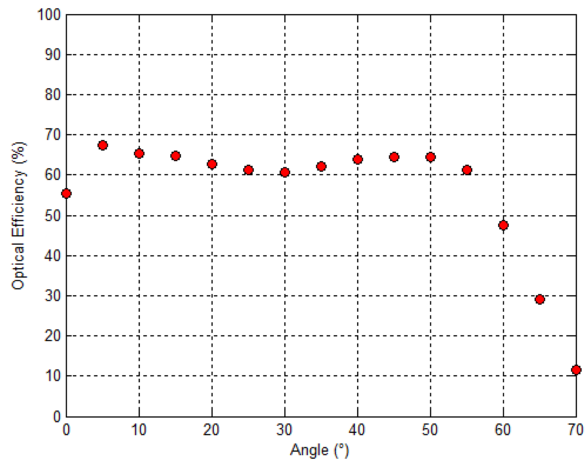

Source: Glint Photonics Inc., 2019.

Table 7: Gen 2 Prototype Performance vs Target Metrics

Metric	Target	Achieved
Aperture Area (sq inches)	16	169 total 37 populated
STC Optical Efficiency	40%	56%
S-ACF (Stationary, Bishop)	25%	63.2%

Source: Glint Photonics Inc., 2019.

Gen 3 Prototype

The project team tested the Gen 3 prototype at incident angles up to 60° under collimated irradiance from a solar simulator. This prototype module included two receiver tiles each with independent electrical connection so that they could be measured independently. Figure 20 depicts the optical efficiency of the outermost tile, and it shows a peak efficiency of 76 percent.

The fill factors of the I-V measurements were high and indicated low internal series resistance within the module. This was validation of the low resistance sliding electrical contacts. The decreasing fill factor with angle reflects the lower absolute irradiance in the solar simulator at higher angles, an indication that the diode behavior of the solar cell is limiting the fill factor, not series resistance.

Table 8 provides a comparison of target and achieved optical performance for the Gen 3 prototype. Note that in this table, the S-ACF value is calculated not from laboratory measurements of optical efficiency (as in previous prototypes) but rather using optical efficiency data extracted from outdoor test data on a clear day. It is therefore more representative of real-world performance.

Figure 20: Gen 3 Module Optical Efficiency Measured Under Solar Simulator

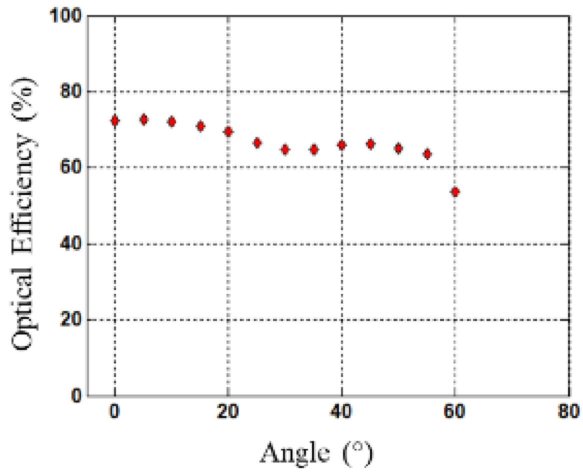

Source: Glint Photonics Inc., 2019.

Figure 21: Gen 3 Module Fill Factor From Solar Simulator Measurements

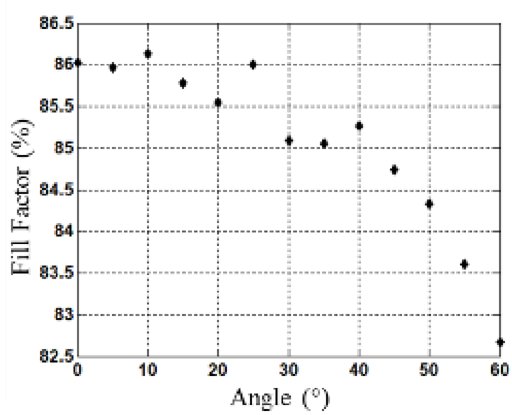

Source: Glint Photonics Inc., 2019.

Table 8: Gen 3 Prototype Performance vs Target Metrics

Metric	Target	Achieved
Aperture Area (sq inches)	144	169 total 37 populated
STC Optical Efficiency	55%	76%
S-ACF (Stationary, Bishop)	45%	59%

Source: Glint Photonics Inc., 2019.

Evaluation of Module and System

System Installation

The project team installed a pilot system involving modules and monitoring hardware on the rooftop of Glint in Burlingame CA and monitored for periods beginning in May 2018. In October 2018, the team installed a Gen 3 module on the rooftop and solar tracking with an applied load was performed autonomously for two months, interrupted once to repair a leak.

Glint is located in a flat-roofed commercial building with a clear horizon to 75° from surface normal. A platform was installed to accommodate racking hardware along with appropriate test equipment. The racking hardware holds the modules azimuthally due south at an adjustable tilt, which was set to latitude tilt (37.7°) for the duration of the testing period. The installation location, mounting hardware, and module are shown in Figure 22.

Figure 22: Pilot System Test Location (left), Mounting Rack (center) and Module (right)

Source: Glint Photonics Inc., 2019.

The module under test contained two photovoltaic tiles, each of which had independently accessible terminals for measurement. All data refers to one tile in the Gen 3 module, encompassing 40 photovoltaic cells connected in parallel under 120 cm^2 of optical aperture area. Efficiency data reported refer to this clear optical aperture area, not the entire module, owing to the significant module area that is not utilized for the tile under test. In a production module at scale, this unused area would be closer to five percent of the module area.

The Keithley 2420 source-measure unit (SMU) monitored the module output, which applied a load to the module and performed periodic I-V sweeps. The SMU was controlled by custom software that held the applied load at the max power point continuously and swept the I-V behavior of the module from short circuit to open circuit once every minute. A four-wire cable was wired from the module to the SMU to perform 4-wire I-V measurements of the 2-terminal module. A motor board controlled by a Raspberry Pi drove the module mechanics. The Raspberry Pi was running custom software that allowed autonomous geopositioning based operation or control via WiFi for closed-loop tracking. Figure 23 depicts the control architecture.

Figure 23: Control Architecture for Pilot System

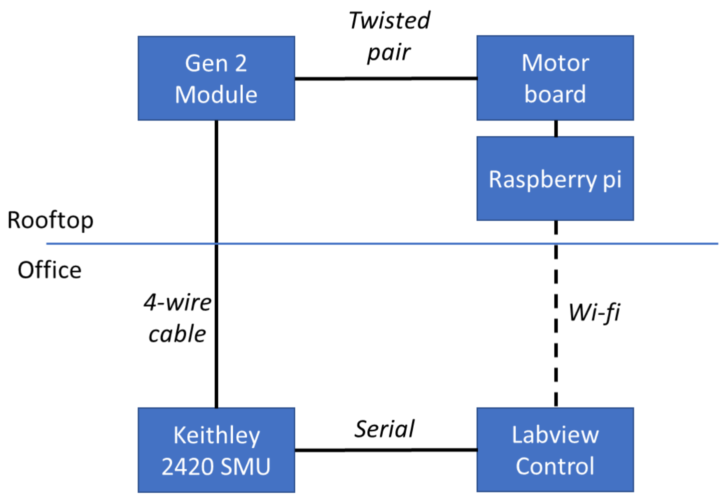

Source: Glint Photonics Inc., 2019.

The system used a closed-loop peak finding algorithm to accomplish solar tracking, whereby the position of the cells was rastered in a spiral and positioned to the point of maximum measured photocurrent. The control system performed the peak finding motion every 10 minutes during daylight hours, and the cells were not moving between these periodic peak findings. This simple algorithm settled upon the focal spot to within approximately two percent of the optimal value, but by overdriving from west to east the natural motion of the sun took the focal spot across the cells and recovered much of that lost two percent. For continuous power production other tracking schemes would be required, but for module measurement this architecture proved robust and simple.

Two additional pieces of test hardware co-located on the roof with the module monitored the ambient conditions. They were an Acurite weather station and a Kipp & Zonen RaZON+ pyroheliometer/shaded pyronameter. The weather station recorded ambient weather conditions, including temperature, wind speed, and humidity, while the RaZON+ recorded incident solar radiation, including both the direct normal irradiance and the global horizontal irradiance.

Data Analysis

Both the maximum power-point tracking (MPPT) and the I-V sweeps recorded the module performance every minute. These data series agree with each other, but as more information can be extracted from the I-V sweeps, the data presented here is derived from the I-V sweeps. The short circuit current is the current extracted from the module when there is zero bias across its terminals and represents the maximum photocurrent the module generates. The short circuit current can be used to determine the optical performance of the module when the response of the photovoltaic cells is well known. A typical I-V sweep is shown in Figure 24 showing the good fill factor obtained with the sliding electrical contact deployed in the Gen 3 modules.

Figure 24: I-V Characteristic of Gen 3 Module Under Solar

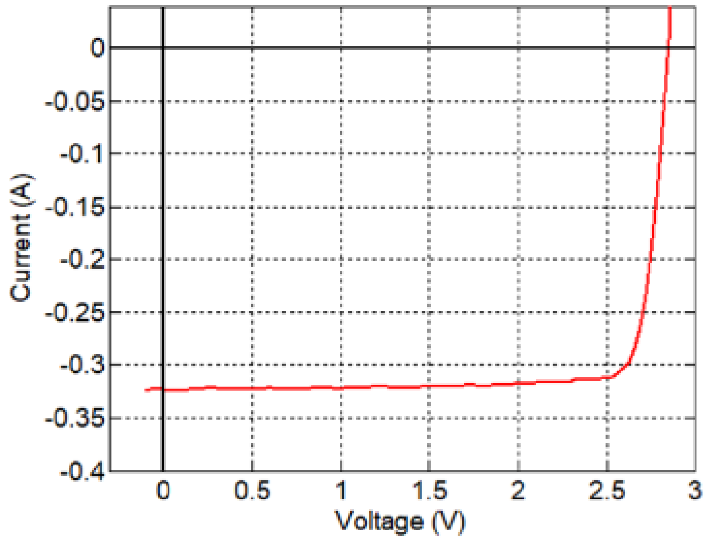

Source: Glint Photonics Inc., 2019.

Figure 25 depicts the short circuit current measured from the module over the course of a clear day during the test. The incident DNI on the plane of the array is plotted on the secondary axes. The relative correspondence between the collected photocurrent at short circuit and the plane of array DNI is the optical efficiency of the module, describing how efficiently the module concentrates the incident DNI onto the photovoltaic cells.

The optical efficiency is defined as the optical power incident on the cells divided by the optical power incident on the optical aperture. It is calculated by assuming a fixed spectral response of the photovoltaic cells and assuming the incident spectrum is the AM1.5D solar spectrum. The team did not collect spectral data during the test, but the effect of spectral changes during the course of a day for a triple junction photovoltaic cell in the optical system was anticipated to be small relative to other sources of error. The optical efficiency is expressed algebraically below, where I_{sc} is the short circuit current, SR is the spectral response of the cells, and DNI_{POA} is the collimated optical power incident on the optical aperture as determined from the measured available DNI and the position of the sun relative to the module.

$$\eta_{Optical} = \frac{P_{Incident\ on\ cells}}{P_{Incident\ on\ lenses}} = \frac{(I_{sc}/SR)}{DNI_{POA}}$$

Figure 25: Short Circuit Current Measured on Pilot System

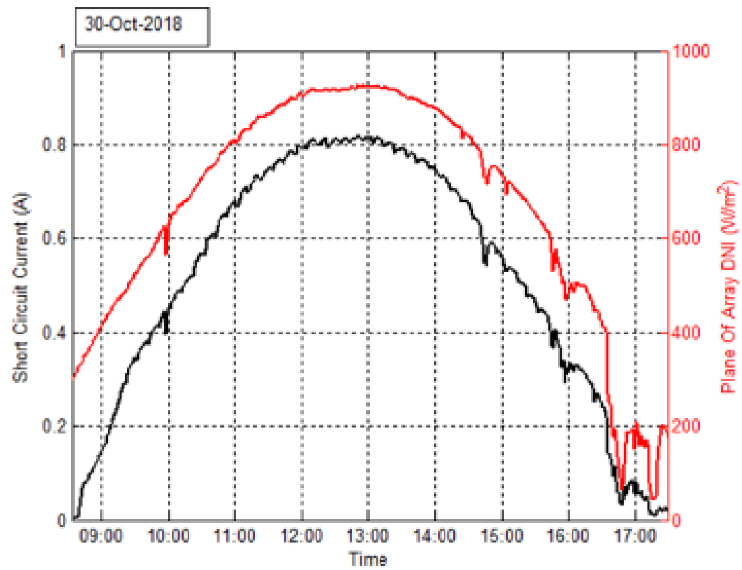

Source: Glint Photonics Inc., 2019.

The optical efficiency over the course of a day is plotted in Figure 26. On the left, the data is plotted as a time series, and on the right is plotted against the incident polar angle between the DNI and the module.

Figure 26: Optical Efficiency of Pilot System

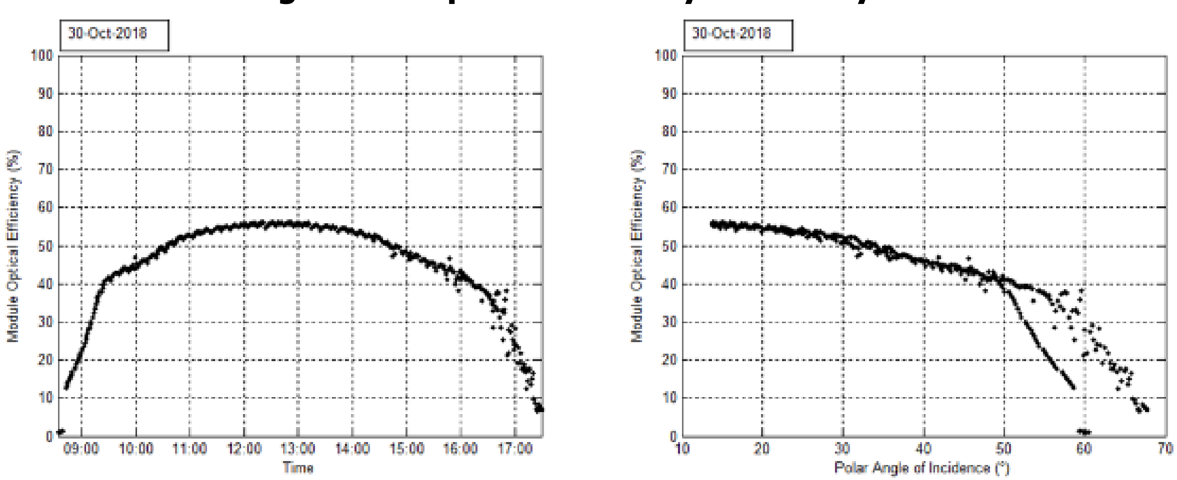

Source: Glint Photonics Inc., 2019.

In addition to the optical efficiency, the power conversion efficiency can be determined from the I-V sweep data. The maximum power point is the electrical load where the maximum power is generated by the module, at the knee of the power generation curve. The power conversion efficiency requires less assumption than the optical efficiency, as the available DNI is directly measured by the pyroheliometer and the power generated is directly measured by the SMU. Figure 27 depicts the power conversion efficiency for the module from the same date, both as a time series and as a function of incident angle.

Figure 27: Power Conversion Efficiency of Pilot System

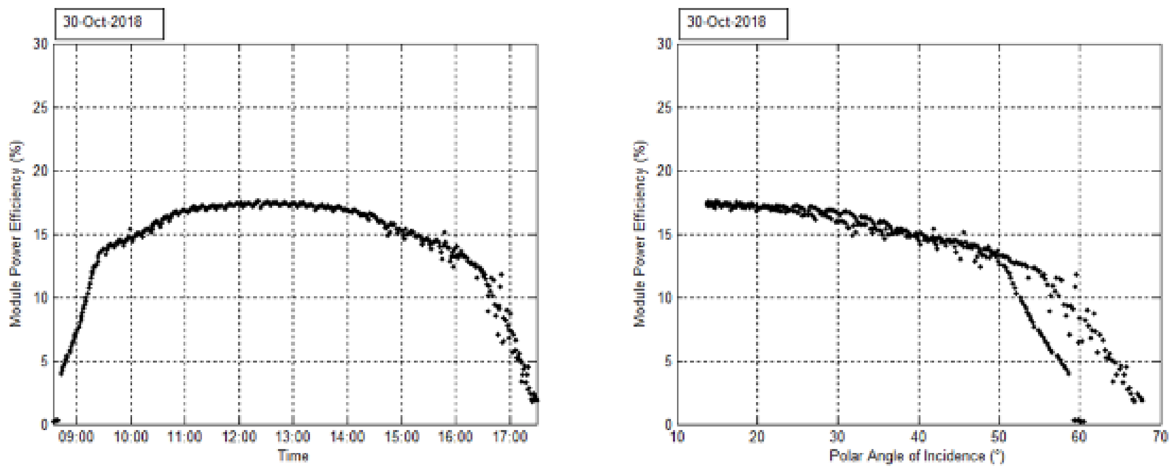

Source: Glint Photonics Inc., 2019.

Figure 28 represents data collected on 10/30/2018, a mostly clear day in Burlingame CA, and accordingly the data series are smooth. On cloudy days there is a source of error inherent in the measurement hardware that must be accounted for. The RaZON+ pyroheliometer that records the available DNI records only 1-minute averages, while Glint's module probed nearly instantaneously every minute. Thus, if the ambient conditions change on sub-minute timescales the module performance cannot be correctly extracted. To account for this, the team applied a screen to the data that disregarded measurements if the two successive measurements were not within 2 percent of its value. This screen is illustrated in Figure 28, with data points that passed the screen circled in red. This eliminated implausibly high or implausibly low data points that result from transient clouds.

Figure 28: Pilot System Test Data from October 30, 2018—Short-Circuit Current, Power Efficiency, and Optical Efficiency

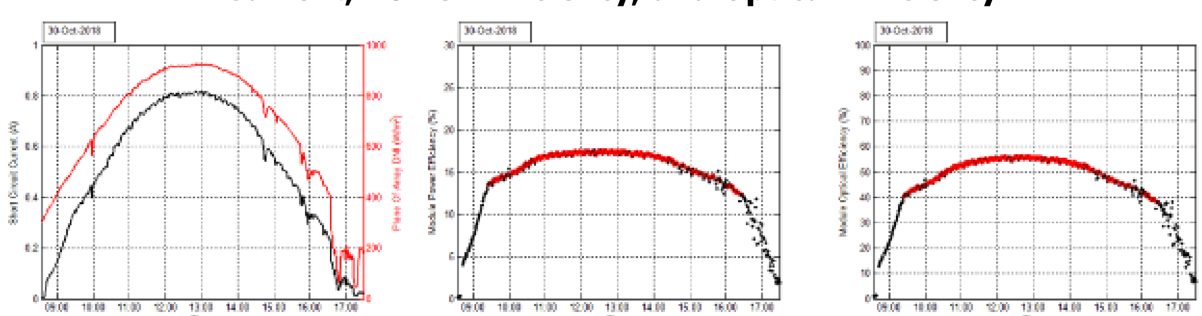

Source: Glint Photonics Inc., 2019.

Finally, the thermal response of the module can be inferred from the I-V sweeps. Circuit modeling of the module was performed using LTspice nodal circuit simulation software. The team used a single-diode lumped circuit element of the photovoltaic cell using parameters from the manufacturer was used to simulate the response of the module under different illumination and junction temperature conditions. This simulation data was then compared to the measured I-V behavior, including the short circuit current and open circuit voltage, to infer an effective junction temperature. Figure 29 shows the calculated junction temperature relative to the measured air ambient temperature as a function of short circuit current is, predictably, a linear relationship, as high photocurrents are generated via greater illumination and power levels.

Figure 29: Calculated Cell Temperature Rise for Gen 3 Module in Pilot System

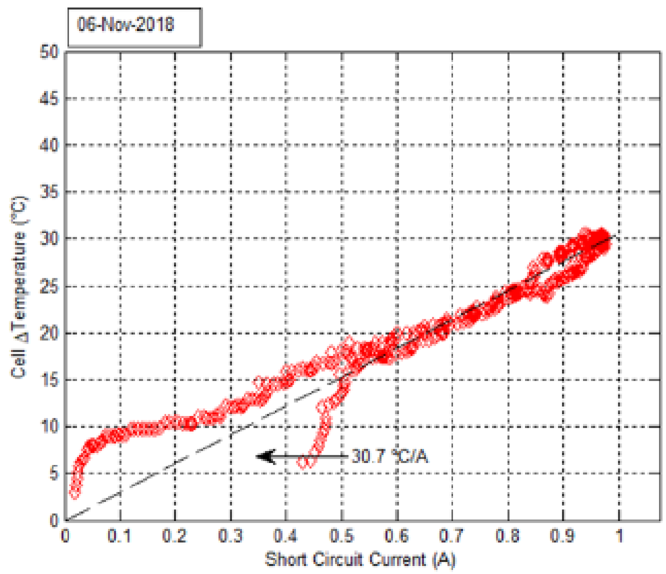

Source: Glint Photonics Inc., 2019.

System Performance

The maximum power conversion efficiency and optical efficiency for each day are depicted in Figure 30.

Days without reported efficiency represent days with too much cloud or smoke cover for reliable measurement, or the period when the module was removed from the roof for re-dosing. The highest power conversion and optical efficiencies were recorded on October 31, 2018 and shortly after, a day when the module was cleaned to remove the dirt that had accumulated during the previous four months of intermittent outdoor testing. These peak efficiencies were >22.5 percent power conversion efficiency and >73 percent optical efficiency for DNI. The bulk of the remaining days exhibited >20 percent power conversion efficiency and >65 percent optical efficiency. The performance of the system under several different types of days is shown in Figure 31.

Figure 30: Daily Peak Efficiency Measured During Rooftop Testing of Pilot System

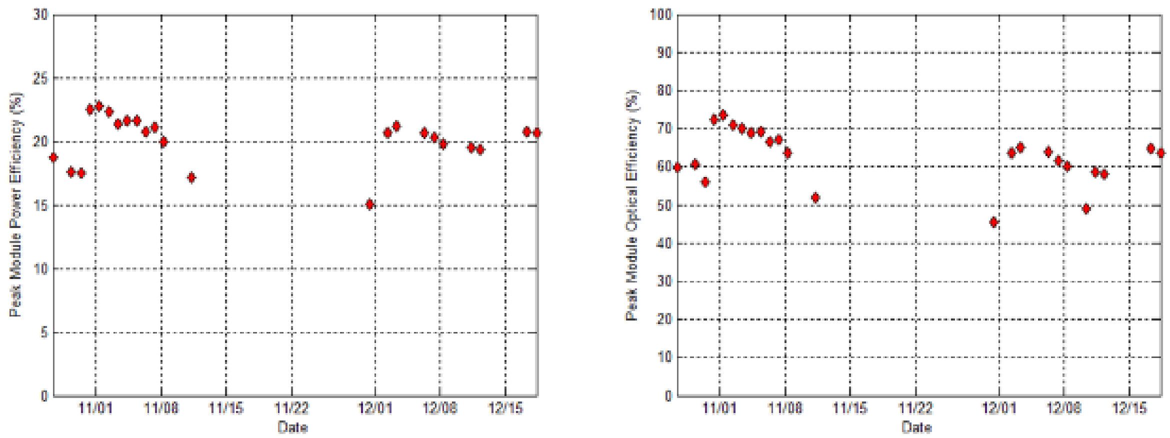

Source: Glint Photonics Inc., 2019.

Figure 31: Pilot System Performance (Short-Circuit Current, Power Efficiency, Optical Efficiency) on Three Days

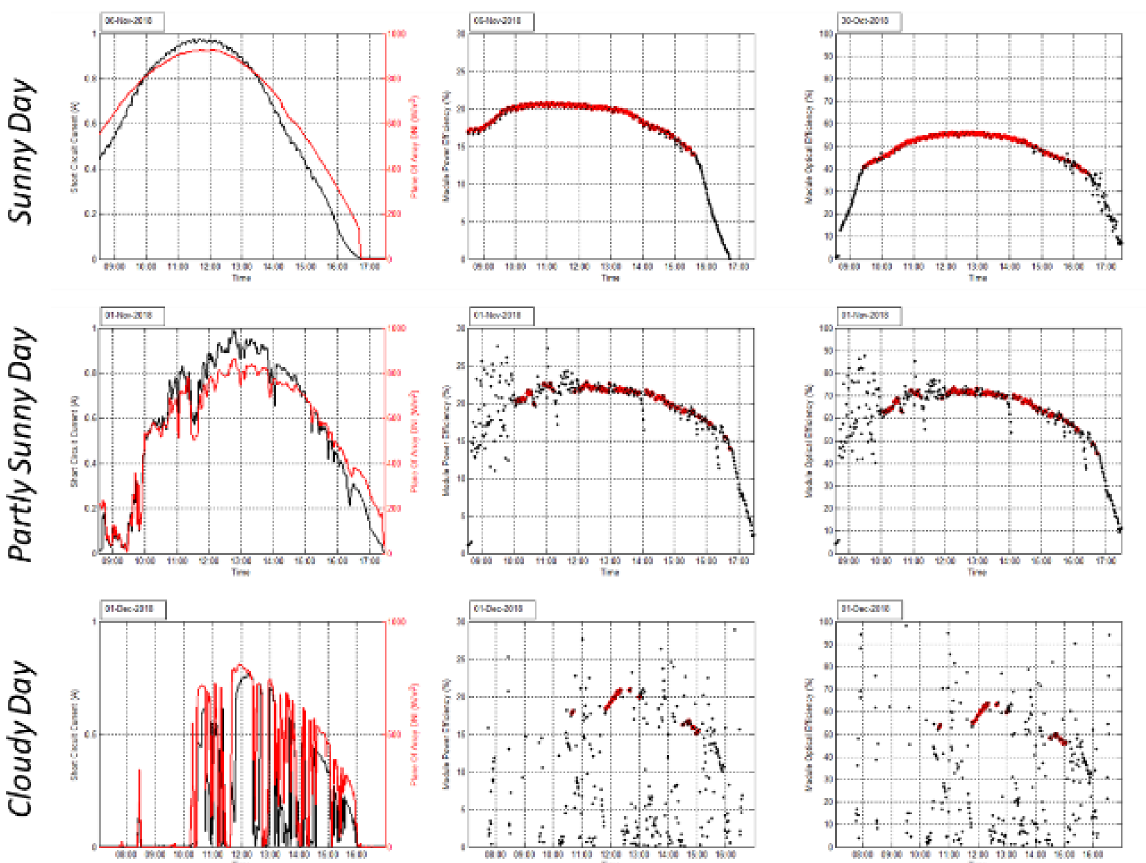

Source: Glint Photonics Inc., 2019.

This testing activities under this project did not undertake a full study of the thermal performance of the modules owing to the limited number of modules under test and the limited availability of sunny days during the test period, but the team collected and analyzed useful data. As described in the previous section, the I-V data could be processed to determine the effective junction temperature of the photovoltaic cells wired in parallel. The slope of the linear fit of that data for each day is plotted in Figure 32 in units of °C/W, representing the cell temperature rise per unit power incident on the cells.

Noteworthy is that prior to 11/9/2018 the cells were left at open circuit between measurements. On 11/9/2018 maximum power point tracking was initiated, and the additional power extracted from the module resulted in a lower steady state operating cell temperature. The impact of heat spreader geometry and ambient weather on the cell temperature, was not explored owing to the limited nature of the system installation.

Figure 32: Daily Cell Temperature Rise with Incident Power

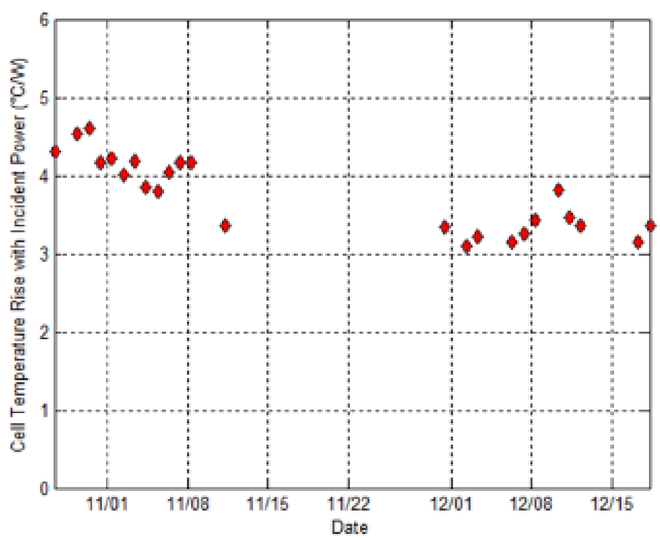

Source: Glint Photonics Inc., 2019.

Third-Party Evaluation

To provide an expert outside evaluation of the measurement procedures, Glint contracted Adam Plesniak of PD3 Consulting to perform a visit and review. Mr. Plesniak is a recognized expert in concentrator photovoltaics, having worked in the field for ten years. He was Director of Research and Development at Amonix, one of the largest CPV companies in the world, where he developed world record CPV modules, and served as Vice President of Products and Engineering at Amonix's successor company, Arzon. He currently works on solar products at Kinematics Manufacturing and Arctica Solar, and serves as treasurer of the American Solar Energy Society. He has served as an expert advisor to a number of DOE programs in the solar field.

Mr. Plesniak visited Glint on November 30, 2018 for the review and evaluation, and spent two hours inspecting the modules and the test and evaluation setup, and discussing the test results. The full report of his visit concludes:

> "*The test set up, data collection and analysis of the Glint self-tracking CPV module seems in all ways to be best practice, thorough and producing expected results from real world outdoor testing*."

CHAPTER 5: Technoeconomic Analysis

Glint developed a suite of performance analysis tools that use TMY datasets collected by the NREL.[2] These datasets are available at 73 locations in California, and the researchers analyzed al the locations. Further, the team analyzed both stationary and single-axis tracked installations in all locations. Some of the assumptions were that the stationary modules were mounted facing south at latitude tilt, and the single-axis tracked installations were mounted on horizontal east-west trackers with a full 180º tracking range.

Cost Model

The project team developed an initial cost model for the CPV modules. This analysis assumed an ultimate module aperture size of 1 m^2. It further assumed a CPV cell cost of $1/$cm^2$ in large volume. This value is well above present costs (~ $5/$cm^2$), but is conservative compared to projections of $0.25/$cm^2$ provided by an NREL analysis (Horowitz, K.A.W, 2015) Optics costs were centered on preliminary discussions with overseas vendors. Most other costs were based on estimates from vendors and discussions with consultants. With a nominal DC module efficiency of 30 percent, these costs come to a module cost of $0.44/W.

Glint used a spreadsheet tool provided by the ARPA-E for the System level costs. Kelsey Horowitz and others at NREL developed the spreadsheet tool, which includes detailed models for balance of solar PV system (BOS) costs and financial assumptions to support the generation of system cost and LCOE estimates. The spreadsheet provides for state-specific LCOE estimation that includes the geographically varying costs for materials, labor, permitting, etc. The spreadsheet further provides for comparison to cost/performance characteristics of incumbent cadmium telluride (CdTe) and monocrystalline silicon (mono-Si) technology. The mono-Si module data is used here as the most relevant competitive comparison point. Unfortunately, the spreadsheet only provides incumbent performance data for three locations: Phoenix Arizona, Kansas City Missouri, and New York City, New York. In the analysis, the team used the Phoenix data as a comparison point. This is because the Glint CPV technology (like all CPV technologies) captures only the DNI solar resource, and so does best in locations such as Phoenix with high DNI (for reference, Figure 33 shows the annual DNI resource in several US locations). The use of this NREL cost model allowed the team to compare

[2] National Renewal Energy Laboratory, National Solar Radiation Data Base, "1991- 2005 Update: Typical Meteorological Year 3"

projected cost/performance of Glint's modules to conventional technologies, using assumptions that have been vetted by NREL as an independent expert body.

Table 9: Assumptions of NREL Spreadsheet Used in LCOE Calculations

Category	Description	Input
PV System Inputs	O&M cost, excluding inverter replacement	$18/(kW_{p(DC)})/year)
	System life	30 years
Financial Inputs	Percent financing from debt	80%
	Percent financing from equity	20%
	Cost of equity	23.1%
	Cost of debt	6.9%
	Loan terms	20 years
Taxes and Incentives Inputs	Rebate: State rebate	0%
	Tax Credit: Federal ITC	30%
	Tax Credit: State Return	0%
	Tax Rate: Federal	35%
	Tax Rate: State	10%

Source: Glint Photonics Inc., 2019.

Figure 33: Available Solar Resource for Various US Cities

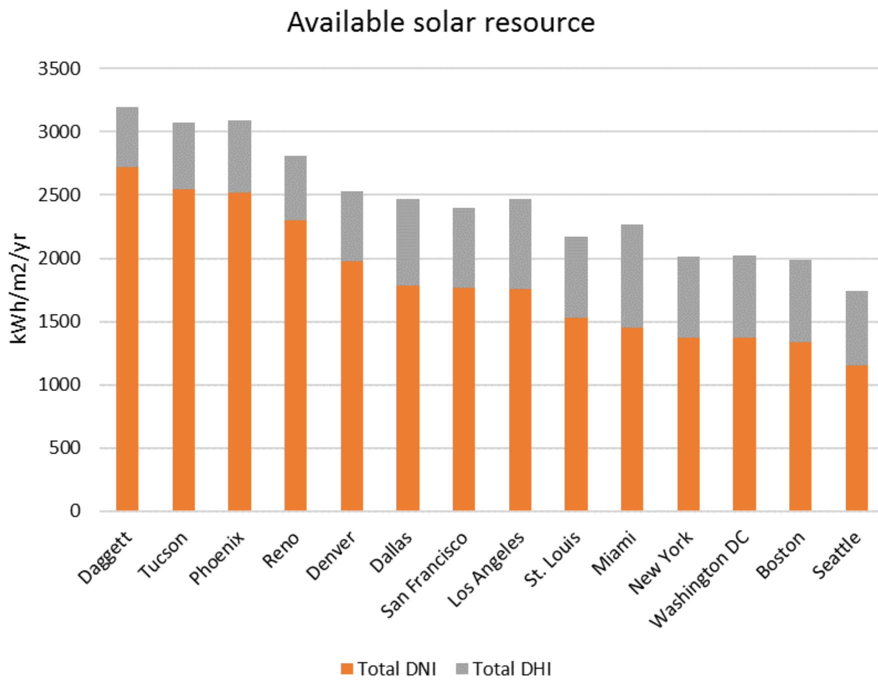

Source: Glint Photonics Inc., 2019.

Performance Model

The team analyzed the module performance with a computational model that predicts annual kWh/m^2 of DC generation for a specific location and mounting, and that includes many factors. The model uses NREL TMY data to determine ambient temperature and incident direct sunlight on an hourly basis. Glint's raytrace optical model is used to determine system optical efficiency as a function of incident light angle in the two primary axes of the panel. The modeled design was further optimized from the Gen 3 optical design, providing optical efficiency that exceeds 85 percent for angles up to 70 degrees as shown in Figure 34. The team developed a finite element computational model to calculate PV cell temperature rise as a function of incident flux on the module. The model estimated real-world PV cell efficiency as a function of cell temperature and incident flux based on published data for a three-junction cell which is very similar to the PV cell used.

Figure 34: Optical Efficiency of Optimized ST-CPV Design

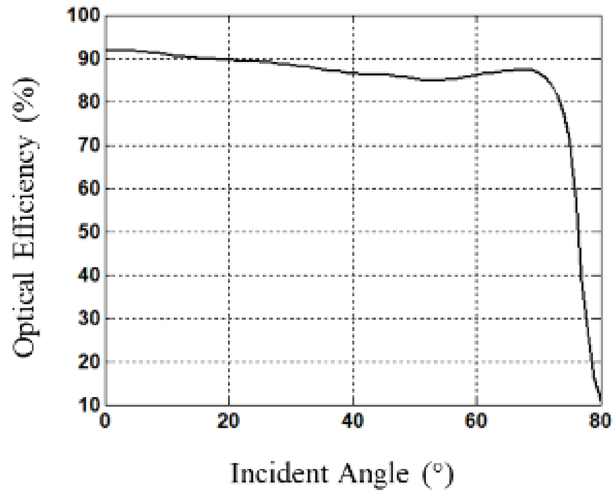

Source: Glint Photonics Inc., 2019.

Appendix A provides the results of cost/performance analysis for stationary and single-axis tracked mounting at the 73 California locations. It shows the annual DNI resource available in each location, as well as predicted AEP, EHE, and LCOE for Glint CPV modules in both stationary rooftop and utility-scale single-axis-tracked configurations. Comparison data for mono-Si was not computed at each location, as a detailed performance model for silicon modules was not available. However, a conservative approach is to benchmark against comparison values generated utilizing high-DNI assumptions.

Finally, Glint noted that while this analysis considers many factors, it is not comprehensive. In particular, it omits several potential sources of loss that are difficult to quantify, such as soiling impact (which affects CPV systems more severely than conventional PV) and loss of aperture area to module framing and mechanics. As a result, the calculated performance should be viewed with some caution.

Cost/Performance Results: Stationary Mounting

For stationary mounting, the calculated EHE exceeds 20 percent in all but one location and reaches as high as 26 percent, indicating a significant performance margin compared to the high-DNI mono-Si EHE of 16 percent. This demonstrates considerable potential for this new technology to deliver the highest possible energy production for area-constrained rooftops.

Further, the team noted that the calculated LCOE values for residential rooftop installations are lower in most locations than the comparison mono-Si value of 11.3 ¢/kWh. This is due to the higher efficiency of the Glint modules, which more effectively leverages the very high and mostly fixed BOS costs for this type of installation. Because BOS costs dominate over module costs for rooftop installations, the LCOE is relatively insensitive to the module cost, providing room to achieve compelling cost/performance even if initial module costs are higher than anticipated. Figure 35 shows the EHE values for Glint CPV modules.

Figure 35: Map of EHE Values for Glint CPV Modules for Stationary Rooftop Mounting

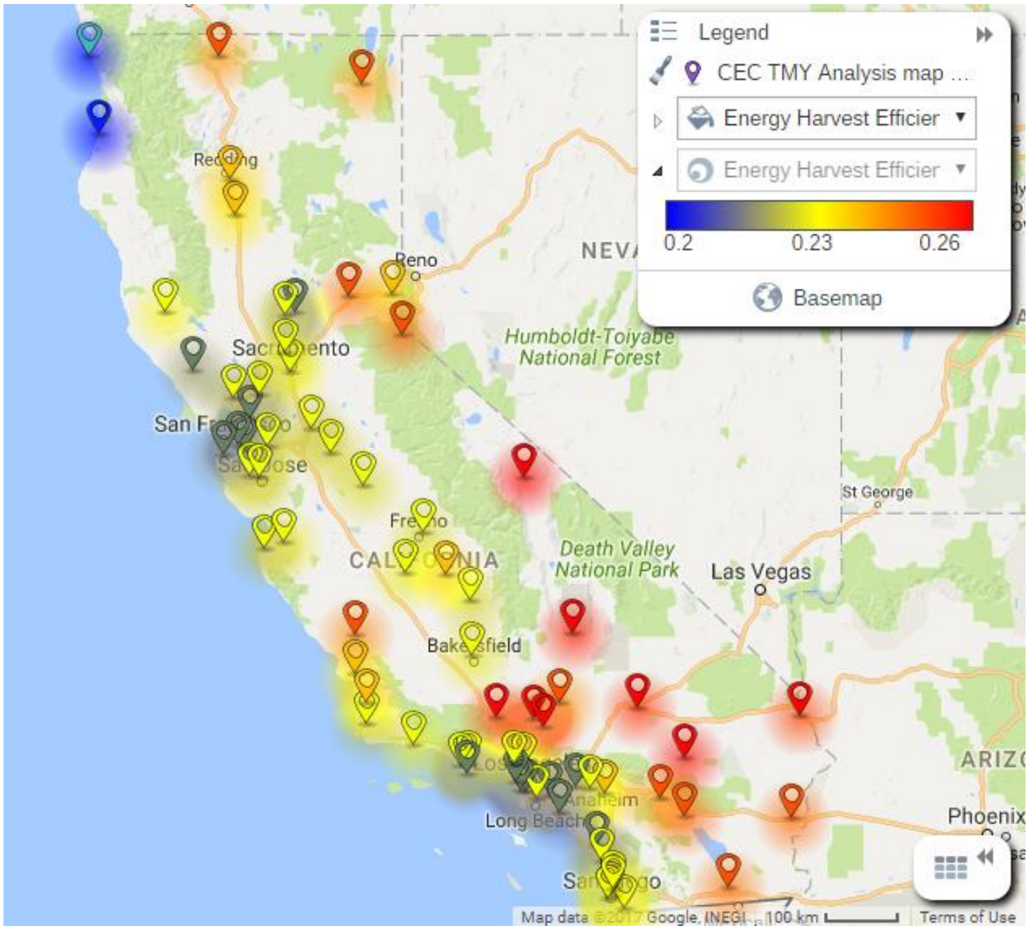

Source: Glint Photonics Inc., 2019.

Cost/Performance Results: Single-Axis Tracked Mounting

For the single-axis tracked case, LCOE is the most meaningful metric. The LCOE values calculated for the utility-scale single-axis tracked mounting case are below the mono-Si comparison of 4.4 ¢/kWh in most locations. In a few select high-DNI locations, the LCOE values dip below 3.5 ¢/kWh, indicating that a 20 percent improvement over mono-Si appeared possible in such locations.

The potential LCOE advantage derives not from low cost modules (the Glint modules are projected to be at least as expensive as mono-Si on a per-Watt basis, even in mass production). Instead, the savings originate in reduced BOS costs. This reduction in BOS costs results from the higher efficiency of the Glint CPV modules compared to mono-Si. At the utility-scale, BOS costs are partly driven by total nameplate power and partly by total area. The Glint modules will allow a more compact installation for a fixed nameplate power. Figure 36 shows the LCOE values for Glint CPV modules.

Figure 36: Map of LCOE Values for Glint CPV Modules in Utility-scale Single-Axis-Tracked Installations

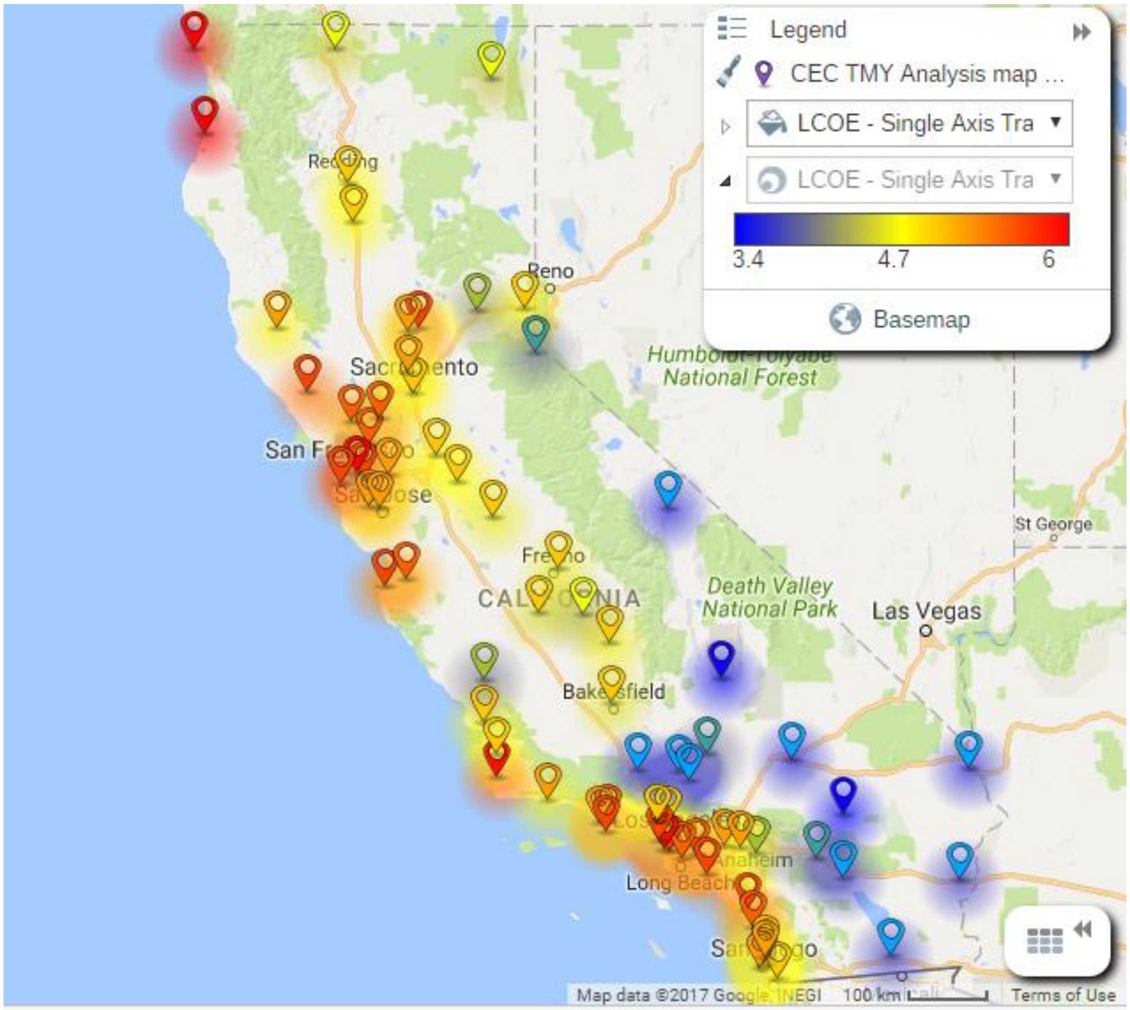

Source: Glint Photonics Inc., 2019.

Overall, this analysis suggests that roof-mounted Glint CPV modules could provide a compelling performance improvement over conventional silicon due to the use of high-efficiency multijunction PV cells. With stationary mounting, the modules might provide up to 26 percent energy harvest efficiency. This high efficiency would be particularly valuable in constrained area applications, such as the rooftops of net-zero-energy buildings.

Achieving a cost advantage over silicon modules is challenging, as commercial module costs continue to fall due to the massive scale that the industry has achieved and the very large investments in manufacturing. The reference module costs used in this analysis date from mid-2017 and are already significantly out of date. Cost estimates for the ST-CPV module in mass manufacturing carry high uncertainty, given the early stage of development. These factors will significantly impede development and adoption of ST-CPV modules for utility-scale markets, and likely in rooftop markets as well.

CHAPTER 6: Technology/Knowledge/Market Transfer Activities

Technology/Knowledge/Market Transfer Work Completed

This chapter lists technology and knowledge transfer activities undertaken during the course of the award. Glint presented the results of the project work in a wide variety of industry and technical forums, including four scientific conferences and two published scientific papers. The research conducted in this project demonstrated the technical feasibility of stationary CPV modules, and Glint will continue to explore opportunities for partnership to commercialize the technology. Further, the research and knowledge developed under this project spawned two product efforts based on related technology.

Oral Presentations on Project Work at Scientific Conferences

- Chris Gladden et al., "Stationary Solar Concentrators: A New Angle on Sunlight," (invited talk) *Conference on Lasers and Electro-Optics (CLEO)*, San Jose CA, May 15-17, 2018.
- John Lloyd et al., "Stationary Catadioptric Concentrating Photovoltaic Modules," *OSA Optics in Solar Energy (SOLAR)*, Boulder CO, November 6–9, 2017.
- Chris Gladden et al., "Stationary Solar Concentrators: A New Angle on Sunlight," (invited talk) *OSA Imaging and Applied Optics Congress*, San Francisco CA, June 26-29, 2017.
- Peter Kozodoy et al., "Toward Stationary Concentrator Photovoltaic Panels," *IEEE Photovoltaic Specialists Conference (PVSC-44)*, Washington DC, June 25-30, 2017.

Booth Presentations at Industry Events

- *ARPA-E Summit*, National Harbor MD, March 13-15, 2018.
- *ARPA-E Summit*, National Harbor MD, February 27-March 1, 2017.
- *ARPA-E Summit*, National Harbor MD, February 29-March 2, 2016.

Scientific Publications

- John Lloyd, Michael Pavilonis, Christopher Gladden, Chadwick Casper, Kevin Schneider, William McMahon, and Peter Kozodoy, "Performance of a Prototype Stationary Catadioptric Concentrating Photovoltaic Module," Optics Express 26, A413-A419 (2018).
- J. Lloyd, P. Kozodoy, C. Gladden, M. Pavilonis, C. Casper, K. Schneider, and W. McMahon, "Design and Prototyping of Stationary Catadioptric Concentrating Photovoltaic Modules," in Light, Energy and the Environment, OSA Technical Digest (online) (Optical Society of America, 2017), paper RW3B.3.

Future Technology Prospects

This project was highly productive, demonstrating technical feasibility of stationary concentrator PV modules and helping to enable a range of follow-on technologies. Glint plans various activities for the continuation of this work, as described below.

1. Continued technology and knowledge transfer for the CPV module technology. Glint anticipates publishing an additional scientific paper summarizing the final results of the project. By continuing to widely share the technical results, the team aim to maximize the opportunity to attract external partners interested in commercialization of this high-efficiency PV technology.
2. Daylighting product development. The technology developed through this program has contributed to Glint’s parallel work developing a solar concentrator panel for building daylighting, as shown in Figure 37. These products use similar optics to collect and concentrate sunlight falling on a stationary panel. The sunlight is then piped into the building interior to provide full-spectrum natural lighting without the use of electricity. The development of daylighting prototypes has been funded by a grant from the Department of Energy, and the technology has attracted interest from companies in the building materials industry. In the coming year, Glint will be continuing development of daylighting prototypes and proving out their performance in pilot installations.

Figure 37: Schematic of Daylighting System, With Photo of Prototype Inset

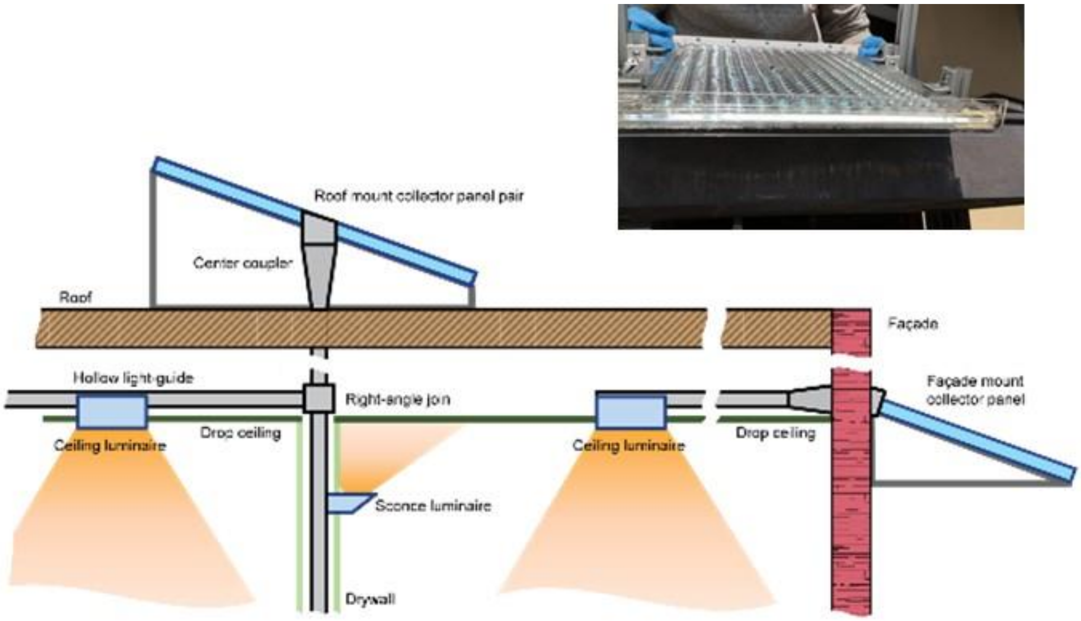

Source: Glint Photonics Inc., 2019.

3. Adjustable LED lighting product development. The technology developed in this project has also contributed to the development of LED lighting products, shown in Figure 38, that use related optical designs. These lighting products provide adjustable beam pointing from stationary fixtures. Coupled with smart controls and sensors, such lighting products can direct light where it is needed, when it is needed, enabling large reductions in electricity use through improvements in the efficiency of light utilization. Development and commercialization of such products is now Glint's primary area of focus. Glint announced the first commercial lighting products this year and will be proliferating to a wide range of fixture products going forward. Glint was selected to receive follow-on funding from the Energy Commission through a Bringing Rapid Innovation Development to Green Energy (BRIDGE) program award to further the development of this novel LED lighting technology.

Figure 38: Schematic of Configurable Luminaire Operation, and Prototype Product Image

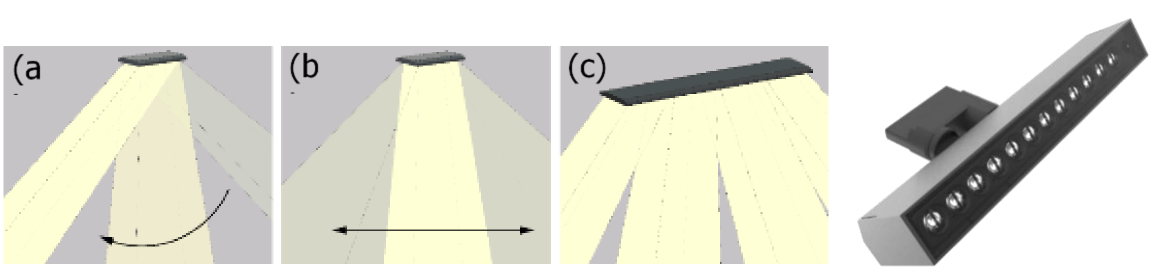

Source: Glint Photonics Inc., 2019.

CHAPTER 7: Conclusions/Recommendations

Conclusions

This project resulted in a number of significant achievements, and successfully met all of the technical performance goals. Through this project, Glint demonstrated an entirely new type of concentrator photovoltaic module. The design is one of the first built for stationary mounting on rooftops, where the high efficiency of CPV has the most value but where previous CPV products have largely been unable to go to the market. Internal microtracking within the module adjusts for the changing angle of incidence, allowing the module to capture sunlight for over eight hours of the day.

During the program, Glint advanced the design of the modules through several rounds of optimization using optical, thermal, and fluidic modeling. Extensive experimental work enabled the production of three generations of prototype modules, each offering improvements in size and performance. Along the way, the team developed new fabrication processes and component designs through many iterative experiments. Each generation of prototypes met or exceeded its efficiency targets, and the team tested extensively the final generation through several months of outdoor rooftop operation.

The final prototype module demonstrated peak power conversion efficiency of 22.5 percent, similar to that achieved by top-performing silicon modules. However, these final prototypes are still early-stage demonstrations that suffer from many known flaws. Analysis of performance potential indicates that optimized modules might provide EHE up to 26 percent in high DNI environments.

Table 10 compares the calculated energy harvest efficiency values of the optimized design (from Appendix A) to the actual performance of the final prototype. For six locations in California, it lists the calculated EHE of the optimized panel and also the actual energy harvest expected from the Gen 3 module in that location, based on its measured performance. The table indicates that prototype performance achieved approximately 62 percent of the optimized performance. This is an impressive performance level for a very early prototype, but also indicates substantial room for improvement. The gap between the calculated values and the achieved ones is due in part to known imperfections of the prototype module, such as incorrect thickness of the optical components, and in part to optical design improvements in the optimized design compared to the lens design that was used in the prototypes.

Table 10: Gen 3 Extrapolated Module Performance

Location	Calculated EHE	Gen 3 Module EHE
Bakersfield	22.7%	14.1%
Bishop	26.0%	15.8%
Burbank	22.9%	14.2%
Long Beach	22.1%	13.9%
Oakland	21.0%	13.3%
San Diego	23.2%	14.5%

Source: Glint Photonics Inc., 2019.

The high efficiency of the modules, combined with their simple stationary mounting, suggests a possibly compelling commercialization opportunity. However, significant market challenges face this new technology in competing against the established mono-silicon module industry. The potential performance advantage of ST-CPV may erode as silicon technology continues to advance. And there is considerable uncertainty around the cost of ST-CPV modules relative to silicon modules. The commercial landscape has changed dramatically during the four year duration of the project, with rapid price reduction for silicon modules that has crowded out most alternative technological approaches. For this reason, the team is cautious about the commercial potential of the ST-CPV approach and recommends that any future development work on the ST-CPV project focus primarily on addressing cost and scalability. The team also recommend that product development be centered on rooftop and other area-constrained applications, where the high efficiency of the ST-CPV approach is particularly valuable.

The novel optical and mechanical architecture developed in this program also has useful application in the lighting field. Glint has spun two new research projects out from this work: one that uses solar concentrator optics to provide daylighting in building interiors, and one that uses similar optics paired with LEDs to provide novel adjustable high-efficiency lighting fixtures. Both of these projects offer substantial energy savings impact, and have strong commercial opportunities due to the design and functionality benefits they offer.

Recommendations

A number of research areas stand out for continued technology development of the ST-CPV module design. Outstanding technical challenges are listed below:

- Module designs to mitigate bowing and ensure accurate vertical positioning of optical elements
- Exploration of manufacturing challenges relating to module scale-up. Larger modules will reduce overall system costs by leveraging motors and mechanics across a larger area

- Cost reduction and simplification of actuators and mechanical design for micro-tracking
- Development of module-scale micro-tracking control circuitry
- More extensive pilot testing and environmental exposure testing
- Critical evaluation of soiling impact
- Detailed cost and performance model development

All of these areas could be addressed with further research and development, if sufficiently funded. Any such work should seek to identify early-entry markets where high efficiency is particularly valued, for example in military use cases. Commercial product development should address rooftop markets first, and only consider utility scale once the technology has matured and costs are well understood. Finding such funding could be a significant challenge, as there is currently little appetite among investors for the risk involved in alternative PV technologies, and especially CPV.

The team recommends that the technology progress be well-documented, so that the learning can be shared and so that development work can be easily restarted should the opportunity arise. This final report serves as one form of documentation. In the meantime, the project team recommends continued outreach and knowledge transfer activities, so that this technical progress can be shared with the wider research community, where it may inspire improvements and future related developments.

Further, Glint recommends aggressive product development of the related spin-out technologies for lighting applications. These products will bring energy benefits of their own, and will also advance the platform understanding for this optical architecture broadly.

CHAPTER 8: Benefits to Ratepayers

Potential Benefits of Self-Tracking Concentrator Photovoltaic Technology

Successful development of ST-CPV modules would bring a number of benefits to California ratepayers. Most fundamentally, the modules could offer a higher-efficiency alternative to existing silicon-based PV panels, enabling greater electricity generation from rooftops and other constrained area locations. This would be a boon to the state's efforts to increase distributed photovoltaic generation and to support net-zero-energy building development. This benefit is particularly pronounced in areas of the state with high direct solar resource.

Total rooftop solar potential for California has been quantified by NREL (Lopez, A., 2012). The team estimated that 50 percent of those rooftops would be appropriate for ST-CPV systems (based on geography as well as roof pitch, etc.), and that in these locations the average direct solar resource is 78 percent of the total solar resource. This yields a potential rooftop installation opportunity of 66 GW, producing 92 terawatt hours (TWh) of electricity annually. This is approximately 40 percent of California's total annual electricity consumption, worth over $11 billion, and therefore represents an enormous opportunity.

Peak solar energy production by ST-CPV systems will also coincide with times of peak demand, meaning that the technology is highly effective at peak demand reduction. The analysis of sky conditions in each climate zone of California during the peak demand periods of 2008 (DEER Update Report, 2008) indicates that 95 percent of peak demand occurred during clear-sky conditions ideal for ST-CPV system operation. Statewide, peak electrical demand is expected to grow to ~ 75 GW by 2020 (CEC, 2009). ST-CPV systems have the remarkable potential to offset 84 percent of this demand if fully adopted on rooftops. Greater adoption of PV power will also reduce greenhouse gas emissions. Full adoption of ST-CPV systems on rooftops would offset 92 TWh of conventional generation, providing an annual savings of 26 million metric tons (CO_2e).

An additional benefit conferred by this technology is an improved energy solution for remote off-grid communities. Many such communities are located in desert areas of California that are particularly well-suited to the use of ST-CPV panels as a result of the high direct solar resource.

Cost savings benefits of the ST-CPV technology are difficult to assess. The technology is at an early stage, so cost estimates for the final product carry significant uncertainty and also will depend strongly on the level of investment in scale-up. Further, the baseline costs of comparison silicon modules has fallen more rapidly in recent years than was anticipated, and the future cost curve is also difficult to predict. The project team believes that the ST-CPV module has the potential to be low cost due to its simple construction and low-cost materials (it is mostly plastic), and considers that with public and private investment it can be competitive with mono-Si on a dollars-per-Watt basis, which would enable a significant market opportunity.

In addition to these benefits, the successful development of this technology will bring significant manufacturing employment opportunities to California. Unlike conventional PV modules which are primarily built overseas, ST-CPV modules are well-suited to local manufacturing because they do not benefit significantly from colocation with the semiconductor foundry. CPV cell technology is an area where US manufacturers have a substantial technical advantage over foreign competitors, including California companies such as Spectrolab and Solar Junction.

Potential Benefits of Related Technologies

Concentrator Daylighting Technology

The ratepayer benefits of a concentrator daylighting product have been analyzed extensively. Indoor lighting represents the largest single component of commercial electricity demand statewide (CEC, 2006), and this use occurs primarily within daytime hours. The substitution of daylighting for electric lighting during sunny days can substantially reduce total electricity demand for lighting, and offers the added benefit of reducing electricity need for Heating, Ventilation, and Air Conditioning (HVAC) systems by eliminating the heat generation associated with electric lighting. The benefits of the technology will be particularly evident during periods of peak demand, which generally fall on hot sunny days. Reducing peak demand will reduce strain on the electrical grid and thereby increase electricity reliability.

The total opportunity for investor-owned utility (IOU) electricity savings in lighting through the use of daylighting systems in commercial buildings is estimated at 1,349 GWh annually, (residential opportunities have not yet been analyzed). This figure derives from separate analyses for each of the 16 defined climate zones in the state, integrating information on office lighting usage and cloud cover. The team used weather reports from the National Climatic Data Center to analyze the weather in each climate zone, assuming that the concentrator would operate with 100 percent efficiency on clear days, 50 percent efficiency on partially-clear days, and 0 percent efficiency on cloudy days (like all concentrators, these devices can only capture direct sunlight). Annual weather efficiency calculated in this way varied from 56 percent to 65 percent across the different climate zones. This weather efficiency was multiplied by the total interior office lighting energy usage in each climate zone (Saxena, 2011) and correction factors of 75 percent for building type (low- and mid-rise buildings only) and 70 percent for hour of the day.

Further electricity-saving benefits accrue from reduction of HVAC requirements when the heating from electric lights is eliminated. Using conversion factors for office daylighting potential, the team calculated the associated potential for HVAC savings at 174 GWh, for a total electricity savings of 1,523 GWh annually. The loss of heating from electric light will create a small increase in the need for gas heat during winter months, which is calculated at 5.18 Mtherms. At the reference rates provided by EPIC, this translates to an overall energy cost-savings potential of $212 million annually and a greenhouse gas reduction potential of 403,000 metric tons annually.

The team calculated a potential reduction in peak electrical demand of 1110 MW, based on an analysis of sky conditions in each climate zone during the peak demand periods of 2008. This total corresponds to 1.9 percent of total peak electrical demand.

Configurable LED Lighting Technology

The configurable LED lighting technology will advance the EPIC goals of lower costs, increased safety, and greater reliability by providing more precise and adaptable illumination in occupied spaces in California and increasing the adoption speed of efficient, long-lasting LED-based luminaires. Glint's dynamically-adjustable lighting technology will allow a better match between light output and lighting requirements, with a resulting increase in end-use energy efficiency, productivity, and safety in lit spaces. This provides higher quality lighting and can save a great deal of energy by improving the targeting of light placement, eliminating excessive illumination. Excessive illumination is wasted electrical generation with all the associated economic and environmental costs of generation and distribution.

Figure 39 shows estimated energy use on a per-luminaire basis for three types of luminaires: (i) conventional LED track light, (ii) Glint manual luminaire, (iii) Glint dynamic luminaire. All cases assume 20W operation at eight hours per day for five years. The dynamic case assumes 60 percent energy savings in targeting and 50 percent energy savings in embodied energy from halving the number of luminaires required.

Figure 39: Energy Benefit of Glint Luminaires

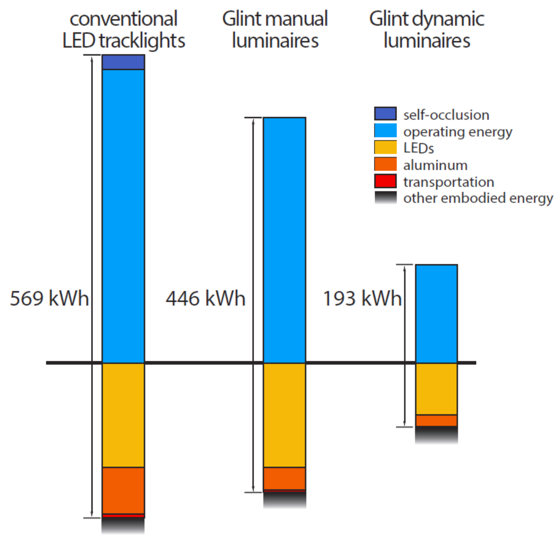

Source: Glint Photonics Inc., 2019.

In their 2016 SSL R&D plan, the DOE highlighted to potential for improving the end-use efficiency of light utilization and estimated a total potential savings of 2x to 3x in use efficiency. This can be estimated from the annual per-capita lighting consumption in the United States of 130.8 Mlmh/yr, (DOE EERE, 2012) equivalent to nearly 16 hours per day of 24 klm. This level of illuminance in a typical field of view is three times greater than the upper end of the recommended range 500 lux for general indoor lighting scenarios. It is difficult to precisely estimate the extent to which this full potential can be realized via adoption of the smart luminaire, but a simple lighting scenario can help illustrate the point. Consider a large indoor space (200 m2) with high ceilings and uniform illuminance levels of 500 lux, consistent with ambient general retail, open office, public lobby, or classroom space. If work surfaces or occupied areas represent 25 percent to 50 percent of the total floor plan. With control over the spatial distribution of light afforded by the smart luminaire, illuminance on these priority areas can be maintained while reducing illumination on other areas such as floors, corridors, or tall furniture, or areas already over-lit via daylight or other fixtures. A 20 percent reduction in illuminance on the over-lit areas, a lumen contrast ratio that would be nearly imperceptible to most people, results in a 10 percent to 15 percent reduction in total lumens and concordant energy consumption. Thus, reasonable estimates for energy savings spans from 10 percent in a very conservative and simple installation, to 70 percent for advanced controllable networks of luminaires.

Additional savings are possible via the potential for more rapid adoption of LED-based directional lighting. The DOE reports that in 2016 12.6 percent of existing lighting installations in the United States utilized LED-based light engines which represent and annual energy savings of 140 GWh (DOE EERE, 2017). Fewer than 0.1 percent of these LED-based lighting installations contained connected controls. The DOE estimated that if these installations featured connected controls the potential energy savings would be an additional 80 percent, representing 110 GWh of energy savings. The increased value and functionality of the configurable luminaire proposed here would increase the adoption rate of connected luminaires, and realize that energy savings.

The extent and value of this potential energy savings can be calculated. Present annual energy expenditures in IOU territories for residential and commercial lighting totals 40.9 TWh. The team estimated that approximately half of this market is addressable by the proposed Glint luminaire, then 20.5 TWh of energy is consumed by lighting fixtures that could be replaced with Glint luminaires. When Glint consider the range of potential energy savings, from 10 percent in the simple, imperceptible scenario described, to upwards of 70-80 percent for advanced controls scenarios envisioned by the DOE, the potential energy savings ranges from two TWh to 16.3 TWh. This amount of potential energy savings corresponds to 662,000 metric tons of CO_2 emissions avoided, worth between $320 million and $2.6 billion per year.

In California there is an additional impact of energy savings through reduced lighting loads in buildings. The climate zones in California are such that reduced electrical loads for lighting in interior spaces improves building energy efficiency by reducing HVAC loads. This effect was estimated to be approximately 13 percent additional energy savings for office buildings in California, and thus an additional 260 GWh to 2.1 TWh of additional electricity consumption can be avoided through synergistic HVAC savings.

Finally, the networked controllable nature of the Glint luminaire, allowing for real time control of the distribution of illumination in space is ideally suited to improving demand response in lighting. In California, Title 24 calls for demand response capabilities in lighting under certain scenarios. The current level of demand response is generally crude zonal dimming capability, with a 15 percent reduction required. The additional control afforded by the Glint luminaire will allow precise illumination tailoring, and larger demand response capacity with less impact.

LIST OF ACRONYMS

Term/Acronym	Definition
ACF	Annual capture fraction. Total annual light captured by the concentrator system and delivered to the solar cells divided by the total direct solar resource available (see chapter 1).
AEP	Annual energy production. Total annual electrical energy (DC) generated per module area (see chapter 1).
ARPA-E	Advanced Research Projects Agency – Energy. A division of the Department of Energy.
AM1.5D	Direct normal component of the air mass 1.5 standard solar spectrum as defined by ASTM G-173-03
BOS	Balance of systems. All elements of a photovoltaic system except the module.
Capacity factor	Actual energy output of a module as a fraction of nameplate capacity (see chapter 1).
Carrier Tray	Component of Glint prototype ST-CPV modules that secure and translate multiple receiver tiles.
Catadioptric	Optical system involving reflective and refractive optical components
CEC	California Energy Commission
CPV	Concentrator Photovoltaics
DC	Direct Current
DNI	Direct Normal Irradiance. Collimated incident solar radiation with an angular width of 5°.
DOE	Department of Energy
EHE	Energy harvest efficiency. Annual energy production divided by total solar resource (see chapter 1).
Fill Factor	The ratio of the maximum power point of a photovoltaic device to the product of the open-circuit voltage and short-circuit current.
Geometric Concentration	The ratio of the area of an optical concentrator to the area on which light is focused.
GWh	Gigawatt Hours

Term/Acronym	Definition
HVAC	Heating, Ventilation, and Air Conditioning
IOU	Investor-owned utility
LCOE	Levelized cost of electricity (see chapter 5)
LED	Light emitting diode
Max power point	The operating bias of a photovoltaic device at which maximum power is generated
MPPT	Max Power Point Tracking. The maintenance of optimal bias on a photovoltaic device under varying conditions.
NREL	National Renewable Energy Laboratory
Open-circuit voltage	The maximum voltage generated by a photovoltaic device at which zero current and zero power is extracted.
Optical concentration	The ratio of the optical power incident on a concentrator to the optical power delivered to the focus of that concentrator. Equal to the geometric concentration multiplied by the optical efficiency.
Photocurrent	Electric current generated by a photovoltaic device.
PV	Photovoltaic
Receiver tile	Component of Glint prototype ST-CPV modules upon which photovoltaic cells are mounted and wired together.
R&D	Research and Development
S-ACF	Annual capture fraction in standard mounting (see chapter 1)
Series resistance	The equivalent resistive load in series with the current source and diode in a lumped circuit diode model of a photovoltaic device
Short-circuit current	The maximum electric current extracted from a photovoltaic device, when zero bias is maintained across its terminals.
SMU	Source-measurement unit test equipment
Soft costs	Costs associated with the non-hardware elements of installation and commissioning of a photovoltaic installation.
ST-CPV	Self-tracking concentrator photovoltaics
STC	Standard test conditions (see chapter 1)
TWh	Terawatt Hours

Term/Acronym	Definition
TMY	Typical meteorological year

REFERENCES

Baker, K; Karp, J.; Tremblay, E.;, Hallas, J.; Ford, J. "Reactive self-tracking solar concentrators: concept, design, and initial materials characterization," Applied Optics 51(8), pp. 1086-1094 (2012).

California Energy Commission. "California Energy Demand 2010-2020 Adopted Forecast," 2009.

California Energy Commission, California Commercial End Use Survey (CEUS) Report (March 2006), Table 8-2, http://www.energy.ca.gov/ceus/index.html

DOE EERE Building Technologies Program 2010 US Lighting Market Characterization – Jan 2012

DOE EERE Report "Adoption of LEDs in Common Lighting Applications" – Jul 2017

Ford, J.E.; Karp, J.H.; Tremblay, E.; Hallas, J.M. "System and Method for Solar Energy Capture and Related Method of Manufacturing". United States of America Patent US2011/0226332, (22 Sept. 2011).

Horowitz, K.A.W.; Woodhouse, M.; Lee, H.; Smestad, G.P. "A Bottom-Up Cost Analysis of a High Concentration PV Module," NREL, 2015.

Karp, J.H.; Tremblay, E.J.; Ford, J.E. "Planar micro-optic solar concentrator" Optics Express 18(2) pp. 1122-1133 (2010).

Lopez, A.; Roberts, B.; Heimiller, D.; Blair, N.; Porro, G. "US Renewable Energy Technical Potentials: A GIS-Based Analysis." NREL Technical Report NREL/TP-6A20-51946, July 2012.

Saxena, Mudit. (Heschong Mahone Group). 2011. Office Daylighting Potential. California Energy Commission.

Price, J. S.; Sheng, X.; Meulblok, B.M.; Rogers, J.A.; Giebink, N.C. "Wide-angle planar microtracking for quasi-static microcell concentrating photovoltaics," Nature Communications, vol. 6:6223, (2015).

Schmaelzle, P.H.; Whiting, G.I. "Lower critical solution temperature (LCST) polymers as a self adaptive alternative to mechanical tracking for solar energy harvesting devices," presented at the MRS Fall Meeting, Boston (29 November–3 December 2010).

Zagolla, V.; Moser, C. "Trackfree planar solar concentrator system" Proc. SPIE 8256, Physics, Simulation, and Photonic Engineering of Photovoltaic Devices, 825618 (February 9, 2012).

Zagolla, V.; Dominé, D.; Tremblay, E.; Moser, C. “Self-tracking solar concentrator with an acceptance angle of 32°” Optics Express, 22 (S7), pp. A1880-A1894 (2014).

APPENDIX A: Modeled Cost and Performance for California Locations

Table A-1: Modeled ST-CPV Cost and Performance
(SRR = Stationary Residential Rooftop, USSAT = Utility-Scale Single-Axis Tracked)

Location	DNI (kWh/m²/yr)	SRR AEP (kWh/m²/yr)	SRR EHE (%)	SRR LCOE (c/kWh)	USSAT AEP (kWh/m2/yr)	USSAT EHE (%)	USSAT LCOE (c/kWh)
Alturas	2280	514	24.2%	10.2	638	26.3%	4.4
Arcata Airport	1323	311	19.2%	16.9	369	21.0%	7.6
Bakersfield Meadows Field	2091	478	22.7%	11.0	617	25.4%	4.5
Beale AFB	1819	415	21.7%	12.6	528	24.2%	5.3
Bishop Airport	2748	623	26.0%	8.4	780	28.1%	3.6
Blue Canyon AP	2306	522	24.6%	10.1	664	27.0%	4.2
Blythe Riverside Co Arpt	2636	595	24.8%	8.8	756	27.1%	3.7
Burbank-Glendale-Pasadena AP	2098	490	22.9%	10.7	610	25.1%	4.6
Camarillo (AWOS)	1933	457	22.2%	11.5	559	24.3%	5.0
Camp Pendleton MCAS	1861	451	21.6%	11.6	534	23.4%	5.3
Carlsbad/Palomar	1907	459	22.1%	11.4	551	24.0%	5.1
China Lake NAF	2830	633	25.7%	8.3	810	28.1%	3.5
Chino Airport	1968	462	21.9%	11.4	568	24.1%	4.9
Chula Vista Brown Field NAAS	2097	498	22.9%	10.5	609	24.9%	4.6
Concord-Buchanan Field	1860	432	21.8%	12.1	545	24.3%	5.2
Crescent City FAA AI	1421	334	20.1%	15.7	399	22.0%	7.0
Daggett Barstow-Daggett AP	2723	617	25.5%	8.5	783	27.8%	3.6
Edwards AFB	2467	557	24.4%	9.4	713	26.8%	3.9
Fresno Yosemite Intl AP	1846	472	22.6%	11.1	610	25.3%	4.6

Location	DNI (kWh/m²/yr)	SRR AEP (kWh/m²/yr)	SRR EHE (%)	SRR LCOE (c/kWh)	USSAT AEP (kWh/m2/yr)	USSAT EHE (%)	USSAT LCOE (c/kWh)
Fullerton Municipal	1846	441	21.4%	11.9	536	23.5%	5.2
Hayward Air Term	1812	432	21.5%	12.2	525	23.6%	5.3
Imperial	2640	596	24.7%	8.8	760	27.0%	3.7
Jack Northrop Fld H	1835	441	21.4%	11.9	529	23.3%	5.3
Lancaster Gen Wm Fox Field	2647	604	25.0%	8.7	764	27.4%	3.7
Lemoore Reeves NAS	2115	485	22.8%	10.8	623	25.4%	4.5
Livermore Municipal	1985	465	22.6%	11.3	579	24.9%	4.8
Lompoc (AWOS)	1767	434	22.1%	12.1	506	23.7%	5.6
Long Beach Daugherty Fld	1860	449	22.1%	11.7	541	24.0%	5.2
Los Angeles Intl Arpt	1763	431	21.1%	12.2	510	22.9%	5.5
March AFB	2316	538	23.7%	9.8	668	25.9%	4.2
Merced/Macready Fld	2061	470	22.6%	11.2	611	25.3%	4.6
Modesto City-County AP	2018	461	22.5%	11.4	596	25.2%	4.7
Montague Siskiyou County AP	2229	503	24.3%	10.4	630	26.6%	4.5
Monterey NAF	1842	441	22.1%	11.9	523	24.0%	5.4
Mountain View Moffett Fld NAS	1950	461	22.5%	11.4	563	24.7%	5.0
Napa Co. Airport	1843	437	22.0%	12.0	541	24.4%	5.2
Needles Airport	2714	610	25.2%	8.6	775	27.5%	3.6
Oakland Metropolitan Arpt	1662	398	21.0%	13.2	482	23.1%	5.8
Oxnard Airport	2012	476	22.5%	11.0	583	24.6%	4.8
Palm Springs Intl	2534	570	24.2%	9.2	725	26.5%	3.9

Location	DNI ($kWh/m^2/yr$)	SRR AEP ($kWh/m^2/yr$)	SRR EHE (%)	SRR LCOE (c/kWh)	USSAT AEP (kWh/m2/yr)	USSAT EHE (%)	USSAT LCOE (c/kWh)
Palm Springs Thermal AP	2660	602	24.9%	8.7	761	27.1%	3.7
Palmdale Airport	2732	622	25.3%	8.4	786	27.6%	3.6
Paso Robles Municipal Arpt	2409	558	24.5%	9.4	699	26.8%	4.0
Point Mugu NF	1846	438	21.2%	12.0	531	23.2%	5.3
Porterville (AWOS)	2052	470	22.5%	11.2	606	25.2%	4.6
Red Bluff Municipal Arpt	2103	478	23.3%	11.0	599	25.6%	4.7
Redding Municipal Arpt	2086	469	23.5%	11.2	596	26.0%	4.7
Riverside Muni	2023	475	22.2%	11.0	584	24.3%	4.8
Sacramento Executive Arpt	2032	465	22.9%	11.3	593	25.4%	4.7
Sacramento Metropolitan AP	2005	457	22.5%	11.5	588	25.2%	4.8
Salinas Municipal AP	1914	460	22.8%	11.4	550	24.6%	5.1
San Diego Lindbergh Field	2030	493	23.2%	10.6	588	25.0%	4.8
San Diego Miramar NAS	2100	500	22.8%	10.5	607	24.8%	4.6
San Diego North Island NAS	1992	480	22.4%	10.9	576	24.3%	4.9
San Diego/Montgomer	2015	479	22.5%	11.0	587	24.6%	4.8
San Francisco Intl AP	1771	421	21.7%	12.5	512	23.8%	5.5
San Jose Intl AP	1952	459	22.5%	11.4	567	24.7%	4.9
San Luis Co Rgnl	2070	488	23.1%	10.7	602	25.3%	4.7
Sandberg	2632	605	25.2%	8.7	767	27.6%	3.7

Location	DNI (kWh/m^2/yr)	SRR AEP (kWh/m^2/yr)	SRR EHE (%)	SRR LCOE (c/kWh)	USSAT AEP (kWh/m2/yr)	USSAT EHE (%)	USSAT LCOE (c/kWh)
Santa Ana John Wayne AP	1798	436	21.1%	12.0	519	22.9%	5.4
Santa Barbara Municipal AP	2028	480	22.8%	10.9	590	25.0%	4.8
Santa Maria Public Arpt	2134	513	23.7%	10.2	617	25.6%	4.6
Santa Monica Muni	1816	436	21.3%	12.0	526	23.3%	5.3
Santa Rosa (AWOS)	1766	413	21.8%	12.7	517	24.2%	5.4
South Lake Tahoe	2442	540	24.9%	9.7	709	27.6%	4.0
Stockton Metropolitan Arpt	2013	458	22.4%	11.4	592	25.1%	4.7
Travis Field AFB	1907	443	22.0%	11.9	551	24.3%	5.1
Truckee-Tahoe	2067	463	23.5%	11.3	600	26.2%	4.7
Twentynine Palms	2853	639	25.8%	8.2	822	28.2%	3.4
Ukiah Municipal AP	2033	463	22.9%	11.3	589	25.5%	4.8
Van Nuys Airport	2122	497	23.0%	10.6	614	25.2%	4.6
Visalia Muni (AWOS)	2190	497	23.5%	10.6	650	26.3%	4.3
Yuba Co	2013	459	22.6%	11.4	587	25.2%	4.8